frontiers in Immunology

ORIGINAL RESEARCH
published: 24 November 2020
doi: 10.3389/fimmu.2020.566476

Host Genetics Background Influence in the Intragastric *Trypanosoma cruzi* Infection

Carolina Salles Domingues[1†], *Flávia de Oliveira Cardoso*[1*†], *Daiana de Jesus Hardoim*[1], *Marcelo Pelajo-Machado*[2], *Alvaro Luiz Bertho*[3,4] *and Kátia da Silva Calabrese*[1]

[1] Laboratório de Imunomodulação e Protozoologia, Instituto Oswaldo Cruz, Fundação Oswaldo Cruz, Rio de Janeiro, Brazil, [2] Laboratório de Patologia, Instituto Oswaldo Cruz, Fundação Oswaldo Cruz, Rio de Janeiro, Brazil, [3] Laboratório de Imunoparasitologia, Instituto Oswaldo Cruz, Fundação Oswaldo Cruz, Rio de Janeiro, Brazil, [4] Plataforma de Citometria de Fluxo, Instituto Oswaldo Cruz, Fundação Oswaldo Cruz, Rio de Janeiro, Brazil

OPEN ACCESS

Edited by:
Wanderley De Souza, Federal University of Rio de Janeiro, Brazil

Reviewed by:
Eden Ramalho Ferreira, Federal University of São Paulo, Brazil
Felix Ngosa Toka, Warsaw University of Life Sciences, Poland

***Correspondence:**
Flávia de Oliveira Cardoso
flaviaoc@ioc.fiocruz.br

[†]*These authors have contributed equally to this work*

Specialty section:
This article was submitted to Microbial Immunology, a section of the journal Frontiers in Immunology

Received: *29 May 2020*
Accepted: *23 October 2020*
Published: *24 November 2020*

Citation:
Domingues CS, Cardoso FO, Hardoim DJ, Pelajo-Machado M, Bertho AL and Calabrese KS (2020) Host Genetics Background Influence in the Intragastric Trypanosoma cruzi Infection. Front. Immunol. 11:566476. doi: 10.3389/fimmu.2020.566476

Background: Considering the complexity of the factors involved in the immunopathology of Chagas disease, which influence the Chagas' disease pathogenesis, anti-*T. cruzi* immune response, and chemotherapy outcome, further studies are needed to improve our understanding about these relationships. On this way, in this article we analyzed the host genetic influence on hematological, histopathological and immunological aspects after *T. cruzi* infection.

Methods: BALB/c and A mice were intragastrically infected with *T. cruzi* SC2005 strain, isolated from a patient of an outbreak of Chagas disease. Parameters such as parasite load, survival rates, cytokines production, macrophages, T and B cell frequencies, and histopathology analysis were carried out.

Results: BALB/c mice presented higher parasitemia and mortality rates than A mice. Both mouse lineages exhibited hematological alterations suggestive of microcytic hypochromic anemia and histopathological alterations in stomach, heart and liver. The increase of $CD8^+$ T cells, in heart, liver and blood, and the increase of $CD19^+$ B cells, in liver, associated with a high level of proinflammatory cytokines (IL-6, TNF-α, IFN-γ), confer a resistance profile to the host. Although BALB/c animals exhibited the same findings observed in A mice, the response to infection occurred later, after a considerable parasitemia increase. By developing an early response to the infection, A mice were found to be less susceptible to *T. cruzi* SC2005 infection.

Conclusions: Host genetics background shaping the response to infection. The early development of a cytotoxic cellular response profile with the production of proinflammatory cytokines is important to lead a less severe manifestation of Chagas disease.

Keywords: *Trypanosoma cruzi*, inbred mice, intragastric infection, host genetic background, proinflammatory cytokines, $CD8^+$ lymphocytes

INTRODUCTION

Chagas' disease is caused by *Trypanosoma cruzi* and it is estimated that there are about 6 to 7 million people infected in the worldwide (1). This parasite presents a great genetic variation and these differences are responsible for a remarkable diversity of isolates, which are classified in seven Discrete Typing Units (DTUs), TcI–TcVI, and Tcbat (2–5).

Since it was described in 1909, Chagas' disease has presented a number of different epidemiological profiles. The evolution of these epidemiological scenarios is due to the various forms of *T. cruzi* transmission, as well as the development of the means used for its prevention. Despite of the progress made to control of infection and the continuous support of a number of organizations, Chagas' disease still affects low-income populations, although has been expanded to North America, Europe, Australia and Japan by migration of million people from endemic countries (6–8). The varied routes of the disease transmission continue to occur, ensuring the continued existence of this zoonosis. However, oral transmission has been showing the main route of infection in the last decades (2, 9, 10).

Outbreaks of acute Chagas disease caused by oral infection have been reported frequently in the Amazon Basin [(11), reviewed by (9)]. Most cases of Chagas disease acquired by oral route were due to TcI isolates, with rare cases involving TcIII and TcIV (12–14). Outbreaks associated with TcII have been reported in southern Brazil (3). Clinical manifestations of Chagas' disease developed after oral infection are more serious than those acquired through the vector pathway. They include acute myocarditis with heart failure, prolonged fever and in some cases, meningoencephalitis (15–17). The disease outcomes depend on several factors such as: both parasite and host genetics, immune response, the route of infection, evolutive forms of the parasite, mixed infections, and cultural and geographical factors (3, 18–22).

Lewis et al. (22) showed the influence of transmission route, evolutive form of parasite and inoculum in *T. cruzi* infection. In this study, 92% of mice infected with 10^4 metacyclic (MT) and 100% of mice infected by intraperitoneal route, with bloodstream trypomastigotes (BT) of *T. cruzi* clone CL Brener exhibited a disseminated infection, with higher parasite loads in the spleen, gastrointestinal tract and adipose-rich tissues. In mice infected intragastrically with 10^4 MTs, about 25% of mice were infected; when the inoculum was increased to 10^5, the infectivity was boosted to 67% and parasites were only detected in the stomach. The mice were not infected with BTs by intragastric route. When oral infection via the oral cavity was realized using 10^4 BT trypomastigotes, 36% of mice were infected, while infection with 10^4 MTs was not transmissible via the oral cavity. When the inoculum was increased to 10^5, infectivity was boosted to 100% in MT infected mice. Parasite load was undetectable in any organ/tissue from animals infected by this route.

A study of our group, using Swiss mice infected intragastrically (IG) or intraperitoneally (IP) by *T. cruzi* SC2005 strain, derived from an outbreak of oral Chagas disease, showed also the influence of route transmission on *T. cruzi* infection. All IP-injected animals showed parasitemia, while just 36% of IG infected mice showed the presence of the parasite in the blood. The parasite load in the blood and mortality rate is greater in mice IP-infected, than in IG-infected mice. The pattern of tissue colonization was the same in both groups of infected mice, regardless of the route of infection, showed great damage in the heart, with the presence of large lymphocytic inflammatory infiltrates (23).

The immune response is another factor that influences the outcome of disease and is determined by the interaction between both parasite and host genetics. Several inbred mouse strains when infected with *T. cruzi* exhibit different profiles of response to infection. Differences in mortality rates, cytokine production, inflammatory infiltrates and parasite load are observed, determining different degrees of susceptibility in the hosts (24–26). CBA mice infected with *T. cruzi* SC2005 strain showed high mortality and parasitemia rates and a Th2/Th17 profile of cytokine production, while C57BL/10 showed lower rates of parasitemia and mortality and a Th1/Th2/Th17 cytokine profile (25). Silva et al. (24) studying the infection by *T. cruzi* Y in several inbred mouse strains (A/J, BALB/c, C3H/HePas, C57BL/6, and DBA mice) also showed differences in mortality and parasitemia rates. A/J mice were the most susceptible to infection, showing the highest rates of parasitemia, mortality, number of inflammatory cells in the liver and number of amastigotes per cell, while the C57BL/6 was the strain less susceptible to infection. In another study, Ferreira et al. (26) observed that BALB/c mice infected by G and CL strains of *T. cruzi* better regulate the immune response than C57BL/6 mice, since BALB/c animals initiated the cytokine secretion earlier. These works demonstrate that factors related to the host genetics are important to control the infection

Studies have been illustrated that the genetic background of the host influence the *T. cruzi* tissue tropism and Chagas disease presentations. Andrade et al. (27) using BALB/c, DBA/2, and C57BL/6 infected by TcI and TcII strains showed that a differential tissue distribution was linked with the MHC variability of the host and no with parasite genetic. Since, BALB/c and DBA/2 mice have the same H-2 haplotype (d) and C57BL/6 mice have H-2 (b) (27, 28). Researches on polymorphisms of some MHC alleles in Chagas' disease patients from Brazil (29); Venezuela (30) and Mexico (31) showed that there is an association between some MHC alleles and disease presentations (32, 33).

Considering the complexity of the factors involved in the immunopathology of Chagas disease, which influence the Chagas' disease pathogenesis, anti-*T. cruzi* immune response and chemotherapy outcome, there is the need for further studies to improve our understanding about these relationships. On this way, the present study used *T. cruzi* SC2005 strain (TcII), isolated from a human case of an oral outbreak of Chagas' disease in the south region of Brazil (34), to infect inbred mice from different genetic backgrounds and to conduct a comparative analysis of the immunopathological, histopathological and hematological profiles, using parameters such as of parasite load, survival rates, cytokines production, macrophages, T and B cell populations frequencies and

histopathology. In this study, we observed that although the infection was disseminated in A and BALB/c mice, A animals were less susceptible to *T. cruzi* SC2005 infection. This lineage developed an early cytotoxic cellular profile, before the increase in parasitemia, leading to a less severe manifestation of Chagas disease.

MATERIAL AND METHODS

Ethics Statement

Experiments were conducted following the guidelines for experimental procedures of the National Council for the Control of Animal Experimentation and approved by the Ethics Committee for Animal Research of the Fundação Oswaldo Cruz (CEUA-FIOCRUZ), license LW 42/14.

Animals

Four to 6 weeks old female mice of the A and BALB/c inbred strains were used in the experiments, provided by Instituto de Ciência e Tecnologia em Biomodelos (FIOCRUZ) and housed under pathogen-free conditions, controlled temperature and food and water *ad libitum*.

Parasites

Trypanosoma cruzi SC2005, belonging to DTU Tc II, was isolated from the peripheral blood of a patient in the acute phase of Chagas disease, acquired orally during an outbreak in Santa Catarina, Brazil, in 2005 (34, 35).

Epimastigote forms of *T. cruzi* SC2005 strain were maintained in LIT (Liver Infusion, Triptose) (AGM) culture medium at 28°C for 21 days, when typically 70%–90% of the parasites had differentiated (36). Metacyclic trypomastigotes were quantified in a Neubauer hemocytometer prior to infection (37).

Experimental Design

A and BALB/c mice were organized into four experimental groups, as follows: Group 1 (G1; n=70): A mice intragastrically infected by 10^7 metacyclic trypomastigote forms of *T. cruzi* SC2005 strain/0.3 ml of LIT medium using a gavage needle; Group 2 (G2; n=70) BALB/c mice, infected under the same experimental conditions as G1; and Group 3 (G3; n=50) and Group 4 (G4; n=50)—control groups, each one composed by uninfected A and BALB/c mice, respectively. In the experimental groups, BALB/c and A mice were submitted to 4 h of fasting prior to intragastric injection. Six animals from each group were euthanized prior to the removal of the blood, esophagus, stomach, gut, heart and liver. Organs were obtained at 7, 14, 21, and 40 days post-infection (dpi). Two independent experiments were performed.

Parasitemia and Mortality

To compare the parasitemia and mortality caused by *T. cruzi* SC2005 intragastric infection between A and BALB/c strains, twenty mice from each group (G1 and G2) were monitored. The parasitemia was determined daily from 5 to 40 dpi. Briefly, 5 µl of blood from each animal's tail vein were collected and placed between slide and cover slip (22 x 22 mm). The number of parasites/ml of blood was estimated by counting 50 microscopic fields in a 400X magnification as described by Pizzi and Prager (38).

The mortality was followed daily until the 50th day after infection. The mortality rate was estimated according to the survival curve generated by the GraphPad Prism 6 program.

DNA Extraction

To quantify the parasite load on the stomach (site of inoculation) and heart throughout the infection in both infected mouse strains, immediately after euthanasia, fragments of both organs (six animals/group) were removed (approximately 100 mg), immediately frozen and stored at—70 °C. After, fragments were digested in 500 µl of lysis buffer (50 mM Tris, 10 mM NaCL, 5 mM EDTA, 0,5% SDS) containing proteinase K (20 mg/ml). DNA was extracted following a standard phenol/chloroform protocol (39).

DNA concentrations and purity were determined by reading A260 and A280 on a NanoDrop 2000c spectrophotometer (Thermo Fisher Scientific, Wilmington, DE, USA).

qPCR Primer Design and Assay Conditions

All primers were designed to be used in a SYBR Green qPCR assay. Primers Cruzi 1 and Cruzi 2 targeting *T. cruzi* genomic DNA sequence (166 bp) and *Actb—actin, beta* (β-actin) mouse gene (138 bp) were synthesized as previously reported (40, 41) (**Table 1**). All primers were manufactured by Gene Link (Hawthorne, NY). The *Actb* reference gene was used as a positive control to monitor DNA integrity, the presence of potential inhibitors of PCR or variation in DNA yield.

All reactions were performed using StepOnePlus Real-Time PCR System (Applied Biosystems). The reaction mixtures contained Power SYBR Green PCR Master Mix 2X (Applied Biosystems), 300 nM of Cruzi1/Cruzi2 or 100 nM of β-actin primers and 25 ng of DNA template in a final volume of 20 µl.

TABLE 1 | Primers used for real-time PCR.

Target	Primer sequence[a]		Sequence source
	Forward	Reverse	
β-actin	AGAGGGAAATCGTGCGTGAC	CAATAGTGATGACCTGGCCGT	X03672/V01217
Cruzi 1	ASTCGGCTGATCGTTTTCGA	–	AY520036
Cruzi 2	–	AATTCCTCCAAGCAGCGGATA	AY520036

[a]*S, C/G.*

PCR conditions were as follows: hold at 95°C for 10 min, followed by 40 temperature cycles of 95 °C for 15 s and 58 °C for 1 min. Standard curves were generated from 10-fold serial dilutions of axenic epimastigotes *T. cruzi* DNA (100 ng – 1 pg). PCR reactions were performed as triplicates for each sample.

A melt curve analysis was performed on all reactions. The quality parameters of the standard curves were analyzed with the StepOne software v2.2.2 (Applied Biosystems).

Histopathology

Histopathological analysis was used to describe the alterations found throughout the infection, in the different organs of infected mice. Following euthanasia, fragments of the esophagus, stomach, gut, heart, and liver of six animals/group were fixed in 4% paraformaldehyde in phosphate buffered saline (PBS), pH 7.45, at 4 °C, for 72 h, cleaved and routinely processed paraffin-embedded. Tissue sections (5μm) were stained with Hematoxylin-Eosin (HE) (Sigma-Aldrich, Sant Louis, USA) technique. The presence of inflammatory infiltrates was classified as: (-) without infiltrates, (+) very mild lesion areas, (++) mild lesion areas, (+++) moderate areas of infiltrates, (+++) severe areas of infiltrates, (++++) very severe areas of infiltrates, follow described by Barreto-de-Albuquerque et al. (42). Tissues were analyzed and photographed under light microscopy (Zeiss, Axioplan 2, with Axiovision LE64 photomicrograph equipment).

Hematological Analysis

Hematological changes occurred after *T. cruzi* SC2005 intragastric infection were determined by the complete blood count (CBC) of six animals/group, in each euthanasia point. The blood was collected by cardiac puncture, placed in EDTA tubes, and sent to the Laborlife clinical laboratory (RJ, Brazil). The blood parameters evaluated were: Red Blood Cell (RBC), Hemoglobin (Hgb), Hematocrit (Hct), Mean Corpuscular Volume (MCV), Mean Corpuscular Hemoglobin (MCH), Mean Corpuscular Hemoglobin Concentration (MCHC), White Blood Cell (WBC) and Platelet (PLT). The CBC was analyzed in an automatic cell counter (Beckman Coulter, Brea, CA).

Cytokine Analysis

Cytokine profile induced by the infection was performed through BD Cytometric Bead Array (CBA) Mouse Th1/Th2/Th17 Cytokine Kit (cat. 560485; BD Biosciences, San Jose, CA) using flow cytometry. Briefly, the detection of TNF-α, IFN-γ, IL-10, IL-6, IL-17A, IL-4, and IL-2 in the serum of animals, was realized using 50 μl of each sample, 50 μl of capture beads and 50 μl of mouse Th1/Th2/Th17 PE detection reagent following CBA-kit instruction guide. Samples were acquired in the BD FACSCalibur flow cytometer (BD Biosciences). The data were analyzed with FCAP Array software (BD Biosciences).

Obtaining of Mononuclear Cells to Flow Cytometry

In the determined euthanasia points, the blood of each animal was collected by cardiac puncture using citrated saline (0.87% NaCl, 3.8% $Na_3C_6H_5O_7$), diluted in the same volume of complete RPMI medium—RPMI 1640 medium (Sigma-Aldrich, St. Louis, MO), supplemented with 10% fetal bovine serum (FBS) (CultiLab, Campinas, Brazil); 200 mM L-glutamine; 100 U/ml penicillin; and 10 μg/ml streptomycin (Sigma-Aldrich, St. Louis, MO), being then added to a Ficoll-Hypaque (Histopaque 1077; Sigma-Aldrich) sedimentation gradient. After centrifugation at 1030 x g for 20 min at 21 C, without brake, the mononuclear cells (MCs) ring was collected.

A lobe of the liver was macerated in 4 ml of complete RPMI medium until complete disruption using a glass tissue homogenizer (Corning E.U.A.), being kept on ice throughout the process.

Cardiac cells were obtained after organ perfusion with PBS (pH 7.2), subsequently cut into small fragments and subjected to four cycles of dissociation using 0.2% type II collagenase in RPMI medium without FBS at 37°C, stirring for 30 min. The supernatant obtained after each dissociation cycle was collected in a single tube and kept on ice.

After obtaining, cells of blood, liver and heart were washed twice (with centrifugation at 720 x g, 4°C, 5 min) in PBS-BSA-(Bovine Serum Albumin) with 10% FBS and resuspended with 3 ml of ACK (Ammonium-Chloride-Potassium) Lysing Buffer, to lyse of red blood cells, incubated for 5 min at RT and washed again. After that, cells were incubated in PBS-BSA with 10% FHS (Fetal Horse Serum) for 30 min, washed again, resuspended with complete RPMI medium and adjusted to $1x10^6$/well.

Flow Cytometry

Flow cytometry was used to quantify the subpopulations of inflammatory cells present in the whole blood (T and B cells), heart and liver (macrophages, T and B cells) of six mice from each experimental group after *T. cruzi* SC2005 intragastric infection.

After each obtaining protocol described above, cells were submitted to flow cytometry staining protocol, consisted by the following monoclonal-antibody panel: anti-CD3-PC7 (Cat 553064; BD Biosciences—maximum emission (max-em): 785 nm) diluted 1:40; anti-CD4-APC-H7 (Cat 560181; BD Biosciences—max-em: 785 nm) diluted 1:80; anti-CD8-BB515 (Cat. 564422; BD Biosciences—max-em: 515 nm) diluted 1:160; anti-CD19-APC (Cat MCA 1439; Serotec—max-em: 661 nm) diluted 1:20 and anti-F4/80-Alexa Fluor® 700 (Cat 123130; Biolegend—max-em: 719 nm) diluted 1:50, in PBS-BSA-FHS. Cells were incubated for 20 min in the dark at room temperature. After washing with PBS, to remove unbound antibodies, the cells were fixed in 1% paraformaldehyde for 30 min in the dark at 4°C, washed and stored at 4°C in the dark until acquisition in flow cytometry. At least 20,000 events from each sample were acquired through CytoFlex flow cytometer (Beckman Coulter). Single stained controls were used to set compensation parameters, while unstained cells were used to set analysis regions. After acquisition, flow cytometric analysis to evaluate the frequencies of $CD8^+$T, $CD4^+$T, $CD4^+/CD8^+$ T, $CD19^+$B, and macrophagic cells were performed using CytoExpert Software (Beckman Coulter). A gate strategy was performed as follows (**Figure S1**): to exclude cell aggregates from analyses, cells were

gated on **Singlets** region in FSC-A *vs* FSC-H dot-plot (**Figure S1A**); from **Singlets** gate an FSC-A *vs* Side-Scatter-Area (SSC-A) dot plot was created and analyses region (mononuclear cells) was defined to encompass mononuclear cells and exclude dead cells from analyses (**Figure S1B**); from **Mono** gate, $CD4^+$ and $CD8^+$ T lymphocytes were determined by CD3 *vs* CD4 and CD3 *vs* CD8 dot plots, respectively (**Figures S1C, D**), CD19+B cells by CD3 *vs* CD19 dot plot (**Figure S1E**) and $F4/80^+$ macrophages by CD3 *vs* F4/80 dot plot (**Figure S1F**). $CD4^+/CD8^+$ double positive T cells was determined by plotting CD8 *vs* CD4 gated on $CD3^+$ (**Figure S1G**).

Statistical Analysis

Data were expressed by mean ± standard error of the mean (SEM) and analyzed statistically by Two-way Anova and Tukey´s multiple comparison post-test. The analyses were performed using the GraphPhad Prism 6 software. Differences were considered significant when $p<0.05$.

RESULTS

Parasitemia and Mortality

All animals of both infected mouse strains presented detectable parasitemia. BALB/c mice showed parasitemia levels significantly higher than A mice, with peaks at 9 and 23 dpi (**Figure 1A**).

Although A mice presented an earlier mortality (16 dpi) its survival percentage was higher, at around 90%, than observed in the BALB/c mice (75%) at 50 dpi (**Figure 1B**).

Parasite Load

The parasite load in the stomach was low in both infected mouse strains. However, both mouse strains showed an increase in the parasite load at 14 dpi, which was significantly higher in A mice than in BALB/c mice, reducing in later times (**Figure 2A**).

In the heart, the parasite load increase at 14 and 21 dpi in both infected lineages. Contrary to observed in the stomach, BALB/c

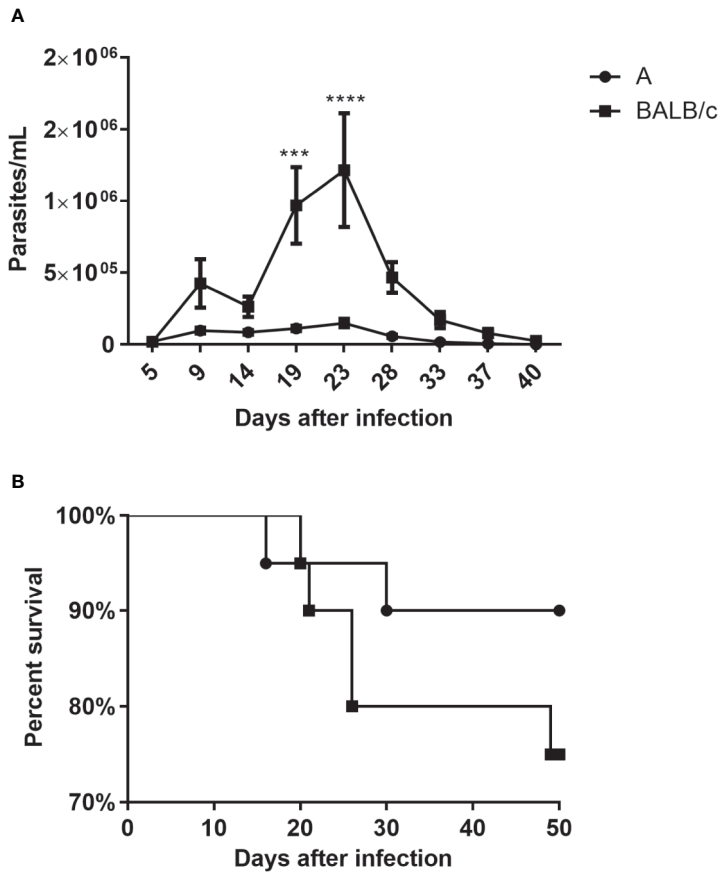

FIGURE 1 | Parasitemia and mortality—A Number of parasites/ml **(A)** and percent survival **(B)** of A and BALB/c mice intragastrically infected by 10^7 metacyclic trypomastigote forms of *T. cruzi* SC2005 strain. Data represent mean ± SEM of two independent experiments with 20 animals/group. Statistical analyses between groups were performed using Two-way Anova and Tukey multiple comparison test. Results were considered significant with $P < 0.05$ (***$P < 0.001$; ****$P < 0.0001$).

mice showed a significantly higher parasite load when compared with A mice, mainly at 21 dpi, however, at 40 days after infection, the parasite load drastically reduce in both strains (**Figure 2B**).

The parasite load in both organs was significantly lower at 40 dpi, when compared to previous moments. In addition, the heart showed a higher quantity of *T. cruzi* DNA in relation to the stomach in both mouse strains (**Figures 2A, B**).

Histopathology

Histopathological analysis of both mouse strains showed similar alterations, with a few modifications in esophagus, stomach, heart and liver throughout the infection. No histopathological alterations were observed in the gut of both infected mice at any time. Neither no alterations were showed in esophagus of infected BALB/c animals during the study. The intensity of inflammatory infiltrates in studied organs was similar in both mouse infected strains, except in esophagus of BALB/c mice, which showed no inflammatory infiltrate. A slight decrease in the inflammatory infiltrate intensity was observed in the stomach (after 21 dpi) and heart (after 14 dpi) of A infected mice (**Table 2**).

Seven days post infection, A infected mice showed a small area of diffuse inflammatory infiltrates in the stomach and heart. In the mucosa, submucosa and muscularis layers of the stomach, mild areas with lymphomonocytic infiltrates were observed (++). The heart showed mild infiltrates in the atrium (++) composed essentially of lymphocytes (**Table 2**). BALB/c mice showed histopathological changes in the stomach, heart and liver.

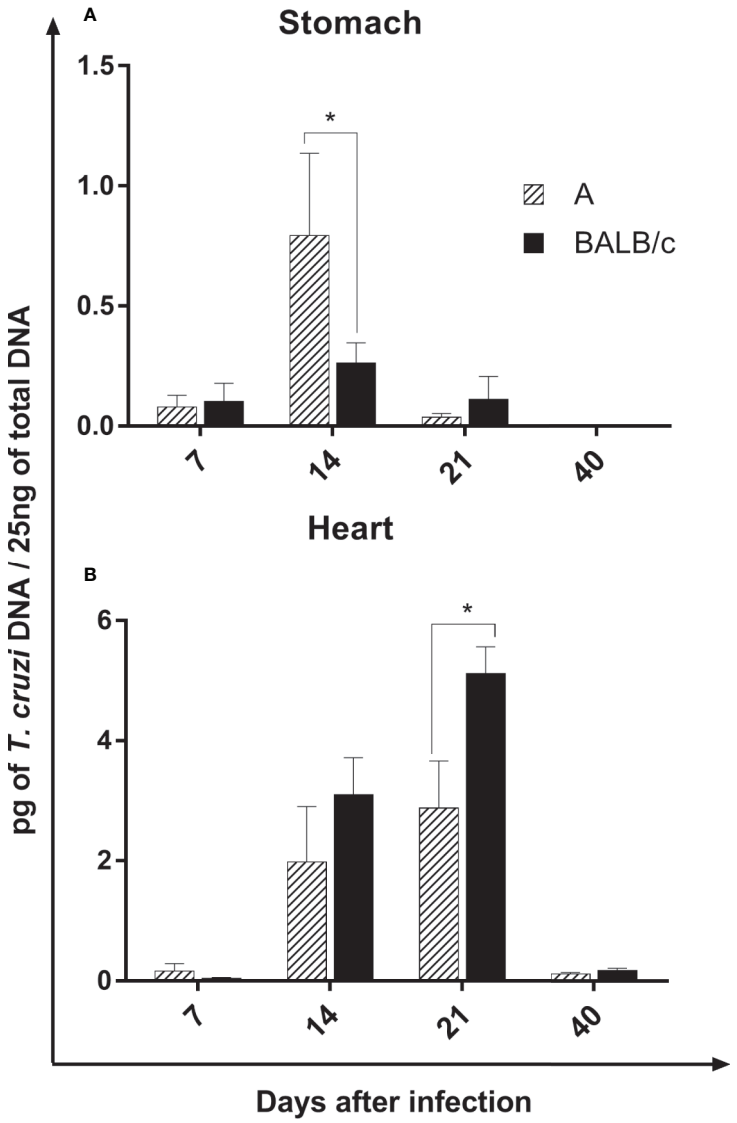

FIGURE 2 | Parasite Load—Quantification of parasites by qPCR in the stomach **(A)** and heart **(B)** of A and BALB/c mice intragastrically infected by 10^7 metacyclic trypomastigote forms of *T. cruzi* SC2005 strain. Data represent mean ± SEM of two independent experiments with six animals assayed in triplicate. Statistical analyses between groups were performed using Two-way Anova and Tukey multiple comparison test. Results were considered significant with *P < 0.05.

TABLE 2 | Semiquantitative analysis of the inflammatory infiltrates in different organs after *T. cruzi* SC2005 infection.

Organs	dpi	Mouse strains	
		BALB/c	A
Esophagus	7	–	–
	14	–	++
	21	–	+++
	40	–	++
Stomach	7	++	++
	14	+++	+++
	21	++++	+++
	40	+++	++
Gut	7	–	–
	14	–	–
	21	–	–
	40	–	–
Heart	7	++	++
	14	++++	+++
	21	+++++	++++
	40	++++	++++
Liver	7	++	+
	14	++	++
	21	++	++
	40	++	++

dpi, days post infection; (-) without infiltrates; (+) very mild lesions areas; (++) mild areas of infiltrates; (+++) moderate areas of infiltrates; (++++) severe areas of infiltrates; (+++++) very severe areas of infiltrates.

Stomach showed mild heterogeneous inflammatory infiltrate (++) in the mucous layer. In the heart, as also observed in the infected A mice, BALB/c mice showed lymphocytic infiltrates in the atrium (++). The liver presented focal and mild inflammatory infiltrate (++), close to the liver portal space (**Table 2**).

As the infection progressed, both mouse strains showed an increase, in the intensity and extent, of inflammatory infiltrates in the different analyzed organs. At 14 dpi, infected A mice exhibited diffuse inflammatory infiltrates of different intensities and distribution in esophagus, stomach and heart. The presence of sparse inflammatory cells was observed in the muscular layers of the esophagus (++). The stomach showed a great circulation of inflammatory cells, with moderate areas of diffuse and intense inflammatory infiltrates (+++), essentially composed by lymphocytes, extended from mucosa to muscular layer, however the inflammatory cells were in greater quantity in muscular layer, which was more affected. (**Figure 3A**). In the heart, the atrium was more inflamed than the ventricle, with an increase in the number of inflammatory cells circulation (+++) and the presence of few *T. cruzi* amastigotes nests (**Figure 3C**). The liver presented small foci of inflammatory cells (++), essentially lymphocytes and macrophages, as well as the presence of megakaryocytes and immature hematopoietic cells (**Figure 3E**). Infected BALB/c mice, showed histopathological changes in stomach, heart and liver. The stomach present moderate areas of diffuse inflammatory infiltrates extended from lamina propria to serosa layer (+++), in the muscular layer biggest areas of inflammatory infiltrates were observed (**Figure 3B**). A moderate inflammatory infiltrate, predominantly composed by lymphoid cells, was observed in the heart, with the atrium being the most affected region (+++). In the ventricle, intense pericarditis, and numerous *T. cruzi* nests were noted (**Figure 3D**). The liver showed moderate and focal inflammatory infiltrates, essentially mononuclear, distributed regularly throughout the organ (++) (**Figure 3F**). Granulocytes, plasma cells and megakaryocytes were noted circulating in the tissue.

At 21 dpi, A infected mice showed areas of moderate diffuse inflammatory infiltrates in the muscular layer of the esophagus (+++). In the stomach, the mucosa, submucosa and muscular layers remained inflamed, but at this point of infection, the tissue damage between the muscle fibers was greater (++++) (**Figure 4A**). The heart showed diffuse inflammatory infiltrates, composed by lymphocytes and plasma cells, between the muscle fibers. The atrium was still more affected than ventricle, with the pericardium and endocardium being the most inflamed regions (++++) (**Figure 4C**). Although the number of inflammatory cells is visually smalls in the ventricle, only in this region were observed *T. cruzi* nests. Examination of liver showed mild areas of focal and heterogeneous inflammatory infiltrate (++), with the presence of immature hematopoietic cells, megakaryocytes and mitosis figures (**Figure 4E**). Infected BALB/c mice stomachs showed a greater tissue damage, with intense and diffuse inflammatory infiltrates (++++). The presence of edema and the separation of fibers from the muscular layers was noticed (**Figure 4B**). At that moment of infection, heart, as well as the stomach, showed more severe histopathological changes. Severe areas of diffuse inflammatory infiltrates were observed in the atrium and ventricle, leading to an injury of muscle fibers, with necrosis and edema (+++++) (**Figure 4D**). Parasite nests were also seen at this time of infection. The liver had mild inflammatory infiltrates, like those seen at 14 dpi (**Figure 4F**).

As the infection progressed, at 40 dpi, the histopathological changes were less intense in both infected mouse strains. Parasite nests were no longer observed in any organs studied and the inflammatory infiltrates observed in the different organs were milder, despite being found in the same regions described previously.

Severe areas of inflammatory infiltrate in the heart and the different cell types observed in the liver of both infected mice, lead us to question about the immune response occurred in these animals. To clarify and justify these findings, it is important to study the hematological changes and cytokines pattern produced after *T. cruzi* SC2005 intragastric infection, as well as characterize phenotypically the cell populations present in the inflammatory infiltrates of affected organs and circulating in the blood, in order to understand the differences in the response to infection between A and BALB/c mice.

Hematological Analysis

CBC revealed a significant reduction in the RBC, Hgb, and Hct at 14 and 21 dpi in the infected mice of both strains, compared to uninfected mice. The decrease in the RBC, Hgb and Hct levels was significantly more pronounced in A mice at 21 dpi and in BALB/c mice at 14 dpi. After this marked decline, the parameters tended to normalize over time (**Figures 5A–C**).

A significative MCV reduction was observed in A infected mice at 14 dpi, only when compared with the control group. At 21 dpi, BALB/c infected mice showed a significant reduction in this parameter, when compared with the control group and A mice (**Figure 5D**).

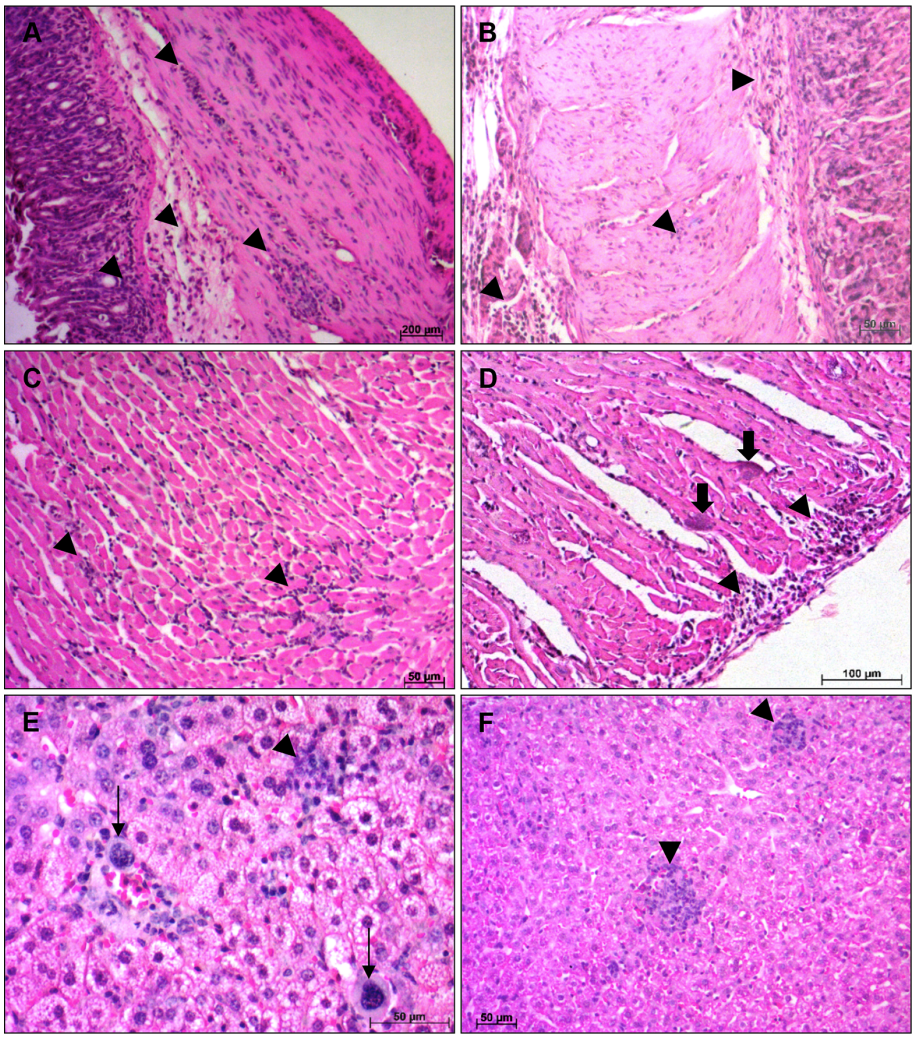

FIGURE 3 | Histological alterations at 14 days post infection—Histopathological alterations in stomach, heart and liver of A and BALB/c mice intragastrically infected by 10^7 metacyclic trypomastigote forms of *T. cruzi* SC2005 strain, at 14 days post infection. **(A)** Lymphomonocytic inflamatory infiltrate (arrowhead), in the stomach of A mice, from mucosa until muscular layer; **(B)** Stomach of BALB/c mice showing inflammatory infiltrates (arrowhead) from mucosa until serosa layer; **(C)** Heart ventricle of A mice with diffuse inflammatory infiltrate (arrowhead); **(D)** Parasites nests (thick arrow) in heart ventricle and diffuse inflammatory infiltrate (arrowhead) in the pericardium of BALB/c mice; **(E)** Lymphocytes, macrophages and megakaryocytes (thin arrow) in the liver of A mice. **(F)** Focal inflammatory infiltrate (arrowhead) in liver of BALB/c mice. Hematoxylin-Eosin (HE) staining method. n = 6 mice/group (three different sections from each mouse).

Alterations in MCH were observed only at 21 dpi in BALB/c infected mice, which showed a significative reduction of this parameter when compared with the control group (**Figure 5E**).

No alterations were observed in MCHC values (**Figure 5F**).

Total white blood cell counts significantly increased in the blood of both infected lineages at 21 and 40 dpi (**Figure 5G**). BALB/c mice showed an increase significantly higher in this parameter than A mice, mainly at 21 dpi. The alteration of this parameter was characterized by an increase of the monocytes and lymphocytes, as well as the presence of a lymphocytic atypia in both infected groups.

Platelet count was significantly reduced only at 7 dpi in A infected mice when compared with the control group (**Figure 5H**).

These results showed that *T. cruzi* SC2005 infection induce an earlier hypochromic anemia (14 dpi), and a higher leukocytosis in BALB/c infected mice at 21 dpi, when compared with A infected mice. This leukocytosis was correlated with the increase of parasitemia in both infected mouse strains.

Cytokine Quantification

Cytokine quantification revealed no changes in IL-10, IL-4, IL-2, and IL-17A cytokines levels. However, TNF-α, IFN-γ, and IL-6 levels were significantly increased in *T. cruzi* A and BALB/c infected mice when compared with the control groups through the infection. Monitoring of these cytokines showed an increase of TNF-α concentrations at 7, 14, and 21 dpi in A infected mice, while in BALB/c infected mice this increase was observed at 14

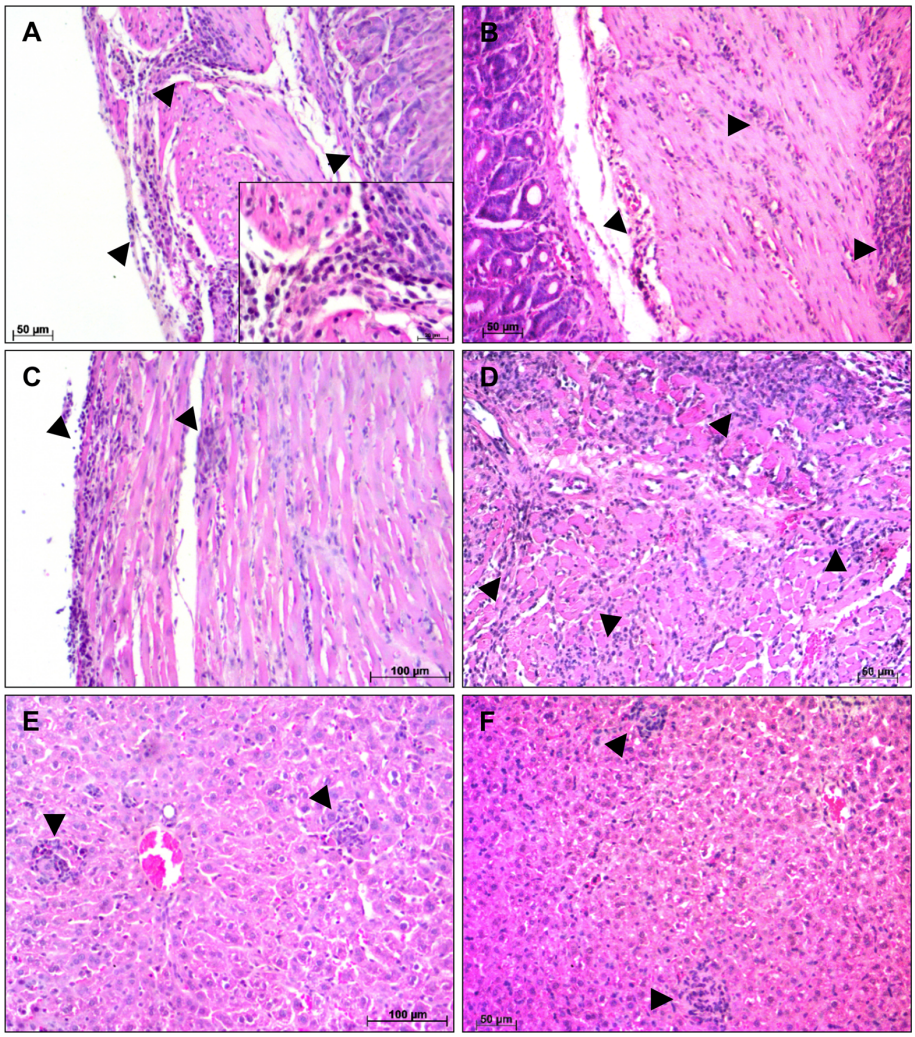

FIGURE 4 | Histological alterations at 21 days post infection—Histopathological alterations in stomach, heart and liver of A and BALB/c mice intragastrically infected by 10^7 metacyclic trypomastigote forms of *T. cruzi* SC2005 strain, at 21 days post infection. **(A)** Stomach of A mice showing a diffuse inflammatory infiltrate (arrowhead), with greater involvement of the muscular layer; **(B)** Lymphomonocytic inflammatory infiltrate (arrowhead) in the stomach of BALB/c mice causing tissue damage in muscular layer; **(C)** Endocardium of the A mice heart showing diffuse inflammatory infiltrate (arrowhead); **(D)** Heart atrium of BALB/c mice with intense inflammatory infiltrate (arrowhead); **(E)** Focal inflammatory infiltrate (arrowhead) in the liver of A mice; **(F)** Focal inflammatory infiltrate in the liver of BALB/c mice. Hematoxylin-Eosin (HE) staining method. n = 6 mice/group (three different sections from each mouse).

and 21dpi, when compared with control groups. TNF-α production was significantly different between infected groups, only at 7 dpi, being higher in A than in BALB/c mice. Both infected groups showed higher levels of TNF-α at 14 dpi (**Figure 6A**).

Increased levels of IL-6 in A mice were found at 7 and 14 dpi, with highest levels detected at 7 dpi. BALB/c infected mice showed increased levels of IL-6 at 7, 14, and 21 dpi, with highest levels at 14 dpi. IL-6 production was significantly different between infected groups, at 7, 14, and 21 dpi, being higher in BALB/c than in A mice (**Figure 6B**).

Both infected mouse strains produced a similar pattern of IFN-γ production, with a significant increase of this cytokine at 14 dpi, when compared to control groups (**Figure 6C**).

These results showed an earlier pattern of inflammatory cytokine production (7 dpi) in A infected mice, when compared with BALB/c infected mice.

Frequencies of $CD4^+$, $CD8^+$, $CD4^+/CD8^+$ T, and $CD19^+$B Lymphocytes and $F4/80^+$ Macrophages

Heart

In this organ an increased circulation of $CD4^+/CD8^+$ T lymphocytes was observed in both infected mouse strains at 21 and 40 dpi. This increase was significantly greater at 21 dpi in A infected mice (17%), when compared with control group and *T. cruzi* infected-BALB/c mice. On the other hand, in infected-BALB/c mice, this increase was significantly greater at 40 dpi, corresponding to 26% of the

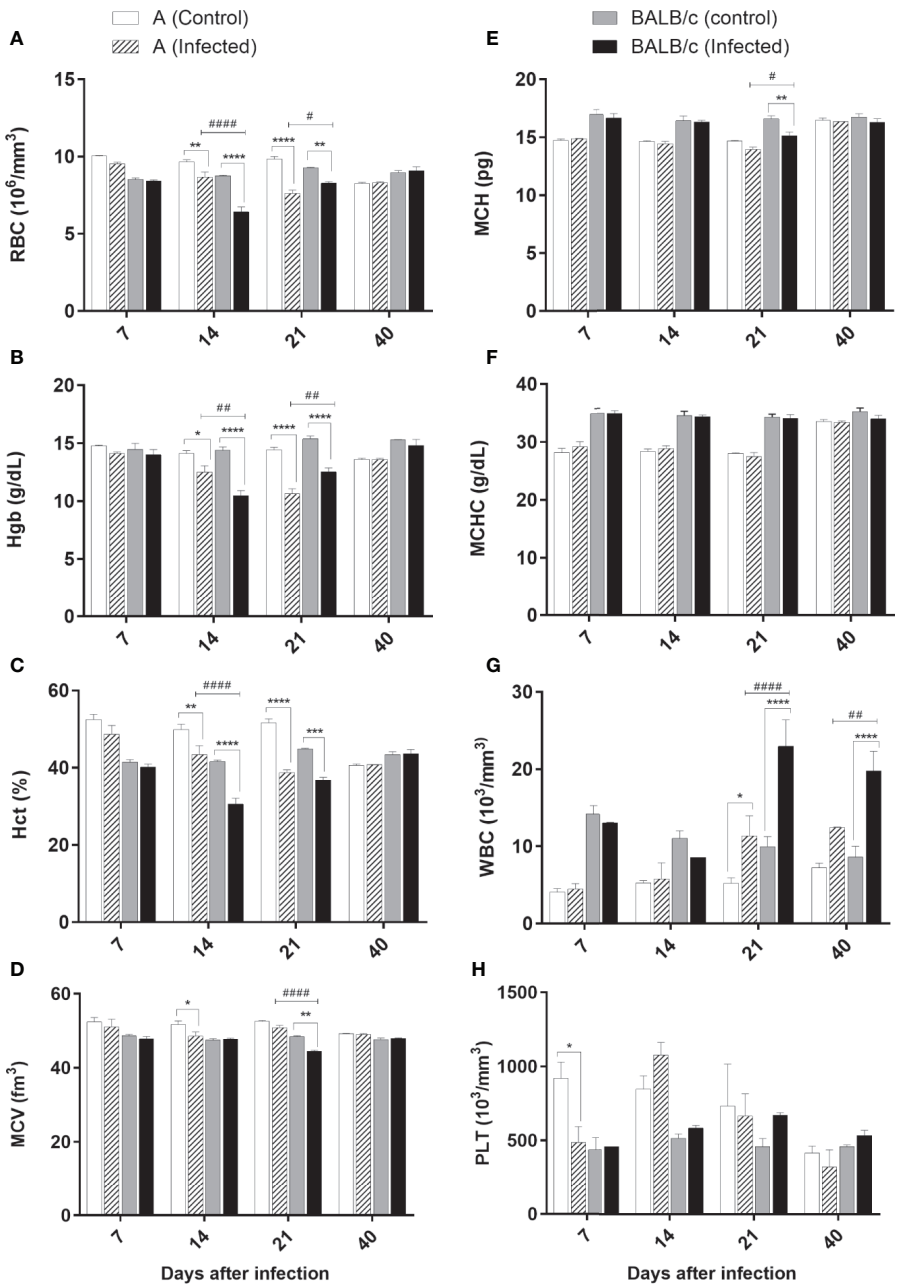

FIGURE 5 | Complete blood count—Complete Blood Count (CBC) of A and BALB/c mice uninfected and intragastrically infected with 10^7 metacyclic trypomastigote forms of *T. cruzi* SC2005 strain. **(A)** Red Blood Cell (RBC) count; **(B)** Hematocrit (Hct) levels; **(C)** Mean Corpuscular Hemoglobin (MCH); **(D)** White Blood Cell (WBC) count; **(E)** Hemoglobin (Hgb) levels; **(F)** Mean Corpuscular Volume (MCV) analysis; **(G)** Mean Corpuscular Hemoglobin Concentration (MCHC); **(H)** Platelet (PLT) count. Data represent mean ± SEM of two independent experiments of 06 animals/group/day. Statistical analyses between groups were performed using Two-way Anova and Tukey multiple comparison test. Results were considered significant with $P < 0.05$ (*$P < 0.05$; **$P < 0.01$; ***$P < 0.001$; ****$P < 0.0001$). * represent differences between infected and control mice, # represent differences between A and BALB/c infected mice.

lymphocyte population, when compared with the control group and *T. cruzi* infected-A mice (**Figure 7A**).

The frequency of $CD4^+$ T lymphocytes subpopulation in the heart from both infected mice strains showed no alteration throughout the study when compared with uninfected groups (**Figure 7B**).

The frequency of $CD8^+$ T lymphocytes increase throughout the infection, showing a large increase in both infected mouse strains, when compared with control groups. In infected A mice, an increase of this subpopulation frequency was observed from 14° dpi to 40° dpi, with the largest increase at 21 dpi. The expansion of this cell type was significantly higher in this strain

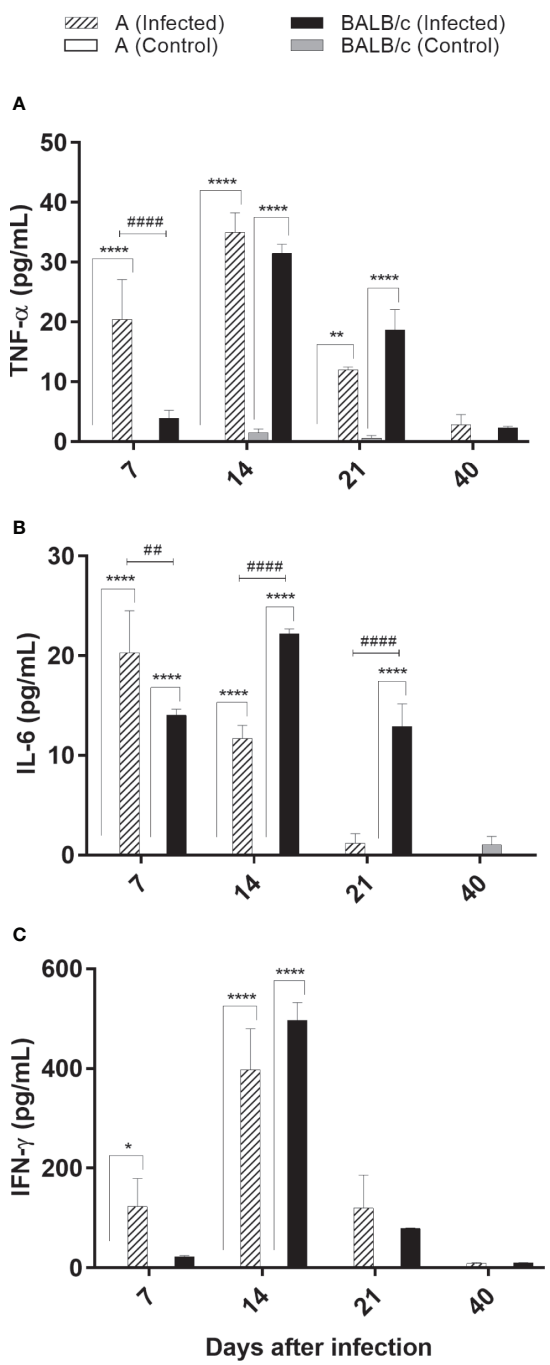

FIGURE 6 | Cytokine evaluations by flow cytometry—TNF-α, IL-6 and IFN-γ levels was assessed in the serum from uninfected and *T. cruzi* SC2005 intragastrically infected A and BALB/c mice. The bars graph representing the mean ± SEM of percentages of **(A)** TNF-α; **(B)** IL-6; and **(C)** IFN-γ produced in the sera harvested from uninfected and *T. cruzi*-intragastrically-infected A and BALB/c mice in the respective time-points: 7, 14, 21, and 40 days after infection. Data represent two independent experiments with 06 animals/group/day. Statistical analyses between groups were performed using Two-way Anova and Tukey multiple comparison test. Results were considered significant with $P < 0.05$ (*$P < 0.05$; **$P < 0.01$; ***$P < 0.001$; ****$P < 0.0001$). * represent differences between infected and control mice, # represent differences between A and BALB/c infected mice.

at 14 dpi when compared with BALB/c infected mice. The expansion of $CD8^+$ T lymphocytes in BALB/c infected mice, was observed at 21 and 40 dpi, with a higher percentage of this population observed at 21 dpi (comprising 36% of the $CD3^+$ T lymphocyte population) (**Figure 7C**). These results showed an earlier expansion of $CD8^+$ T lymphocytes after *T. cruzi* SC2005 intragastric infection in A infected mice, when compared with BALB/c infected mice.

Quantification of $CD19^+$ B cells was lower and similar throughout the experiment in both mouse strains, with exception of a reduction in the frequency of these cells in A infected mice, at 14 dpi, and in BALB/c infected mice at 21 dpi when compared to uninfected groups (**Figure 7D**).

Similar to observed in $CD4^+$ T lymphocytes, the percentage of $F4/80^+$ macrophages was similar to the respective control groups in both mice infected strains (**Figure 7E**).

Liver

Distribution profile of $CD4^+/CD8^+$ T cells in the liver showed a significative increase of these cells in A infected mice, at 14 dpi (comprising 5% of the lymphocyte population), when compared with the control group and BALB/c infected mice. On the other hand, in BALB/c infected mice this increase was observed at 21 and 40 dpi, when compared with the control groups, but not significantly different of A infected mice (**Figure 8A**).

$CD4^+$ T cell subpopulations was significantly decreased in both mouse strains at 14 dpi, and at 21 dpi in BALB/c infected mice when compared with the control groups. Nevertheless, these differences were not significant between infected groups throughout all experiment in this organ (**Figure 8B**).

Contrary to observed in $CD4^+$ T cells subpopulations, $CD8^+$ T cells frequency increased from 14 dpi in animals infected by *T. cruzi*. An expressive increase of this cell type was observed at 14, 21, and 40 dpi in infected A animals, ranging from to 11% and 15% from $CD3^+$ T lymphocyte population. In BALB/c infected mice this increase was significant at 21 and 40 dpi, reaching almost 20% at 40 dpi (**Figure 8C**).

A infected mice showed an expansion of $CD19^+$ B lymphocytes at 14 and 21 dpi. The percentage of these cells was two-fold higher in the infected mice than observed in the controls and BALB/c infected mice at 14 dpi (**Figure 8D**).

The frequencies of $F4/80^+$ macrophages declined significantly in A mice only at 14 dpi, when compared with control group (**Figure 8E**).

Blood

The evaluation of the $CD4^+/CD8^+$ T cells in the blood exhibited the same pattern in both infected groups, showing a significant difference between infected mouse strains only at 14 dpi. In A infected mice, there was a significant increase of these cells at 14, 21, and 40 dpi (ranging from 24% to 30% of the T lymphocyte population), while in the BALB/c infected mice, this increase was significant at 21 and 40 dpi (24% and 28% of the T cell, respectively) (**Figure 9A**).

$CD4^+$ T lymphocyte kinetics indicated a significant reduction of this subpopulation in both infected mouse strains at 21 and 40

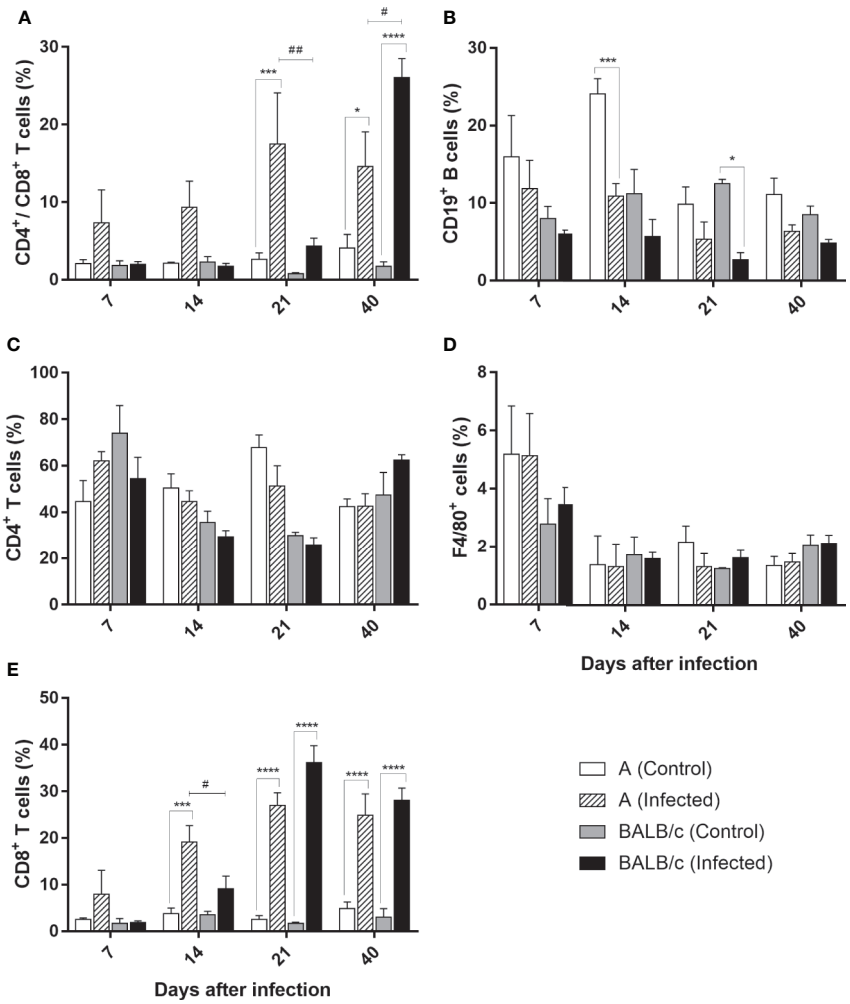

FIGURE 7 | Flow Cytometry analysis of the heart - Frequencies of $CD4^+/CD8^+$ T lymphocytes **(A)**, $CD19^+$B lymphocytes **(B)**, $CD4^+$T lymphocytes **(C)**, F4/80+ macrophages **(D)** and T $CD8^+$ T lymphocytes **(E)** in heart samples obtained from uninfected and T. cruzi SC2005 intragastrically infected A and BALB/c mice. Data represent mean ± SEM of two independent experiments with six animals/group/day. Statistical analyses between groups were performed using Two-way Anova and Tukey multiple comparison test. Results were considered significant with $P < 0.05$ (*$P < 0.05$; **$P < 0.01$; ***$P < 0.001$; ****$P < 0.0001$). * represent differences between infected and control mice, # represent differences between A and BALB/c infected mice.

dpi, when compared with control groups. These reductions were significant between infected mouse strains only at 40 dpi (**Figure 9B**).

$CD8^+$ T cells exhibited the same pattern observed in the $CD4^+/CD8^+$ T cells, in both infected groups, with a significant difference between infected mouse strains only at 14 dpi. $CD8^+$ T cells increased from 14 dpi in A infected mice. An expressive increase of this cell type was observed at 14, 21, and 40 dpi in this group, ranging from 35% to 44% of the $CD3^+$ T lymphocyte population. In the BALB/c infected mice this increase was more significant at 21 and 40 dpi, reaching almost 49% of the total of T cells (**Figure 9C**).

A reduction in the $CD19^+$ B cells was observed in the blood of the animals throughout infection. A infected mice presented an expressive decrease at all the points studied. At 21 dpi the percentage of $CD19^+$ B lymphocytes in the infected animals was nearly seven-fold lower than observed in uninfected mice. Likewise, BALB/c infected mice exhibited a significant reduction in this population through the infection, however, more significant at 21 and 40 dpi. At 21 dpi the reduction was more pronounced, and an average of 6.68% of $CD19^+$ B cells was observed among BALB/c infected animals, while the control group had a population of around 28% (**Figure 9D**).

DISCUSSION

Clinical outcomes of Chagas's disease depend on the complexity of the factors involved, related both to the parasite (genetic

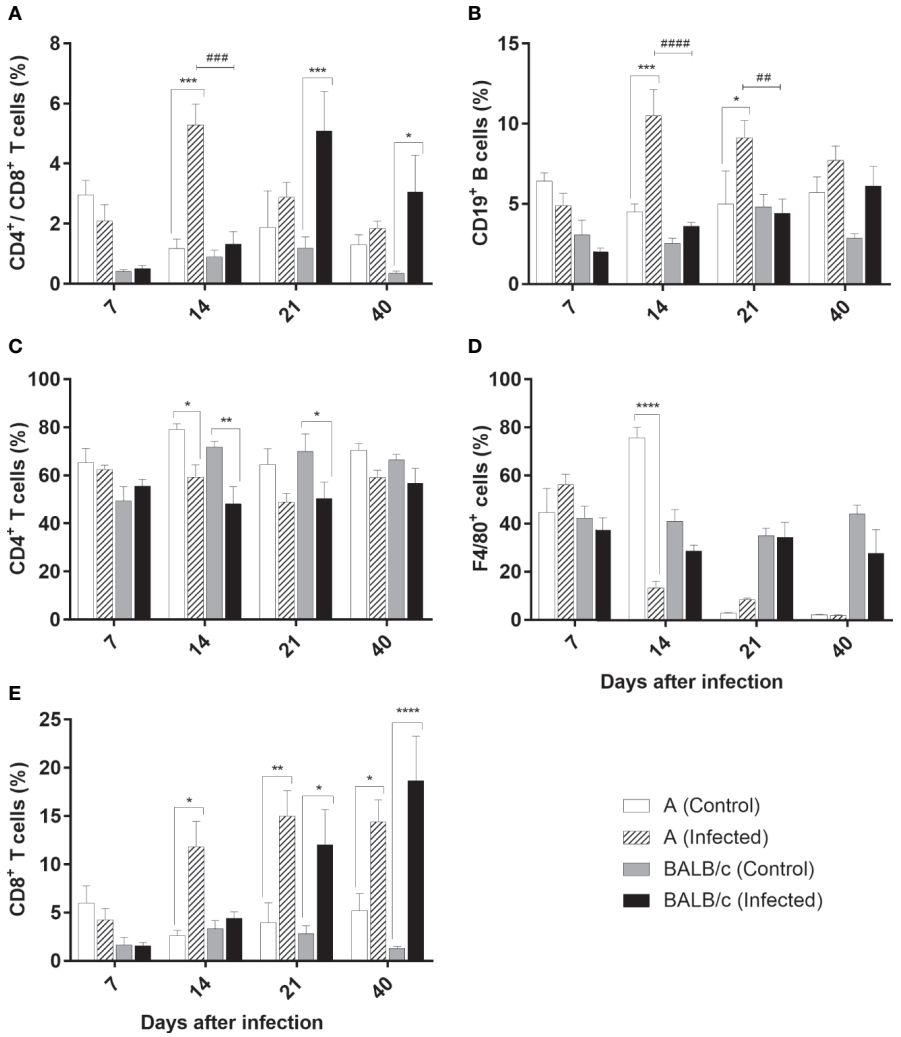

FIGURE 8 | Flow Cytometry analysis of the liver - Frequencies of $CD4^+/CD8^+$ T lymphocytes **(A)**, $CD19^+$B lymphocytes **(B)**, $CD4^+$T lymphocytes **(C)**, $F4/80^+$ macrophages **(D)** and T $CD8^+$ T lymphocytes **(E)** in liver samples obtained from uninfected and T. cruzi SC2005 intragastrically infected A and BALB/c mice. Data represent mean ± SEM of two independent experiments with six animals/group/day. Statistical analyses between groups were performed using Two-way Anova and Tukey multiple comparison test. Results were considered significant with $P < 0.05$ (*$P < 0.05$; **$P < 0.01$; ***$P < 0.001$; ****$P < 0.0001$). * represent differences between infected and control mice, # represent differences between A and BALB/c infected mice.

variability, inoculum, infectivity, pathogenicity, virulence, and inoculation pathways) and to the host (age, sex, nutrition, immune profile, and species). The interactions between these factors exert a crucial influence on the pathophysiology of Chagas disease, interfering in the host's immune response and in the evolution of the disease (21, 27, 32, 33, 43).

The route of infection is considered an important factor for the occurrence of disease and a determinant of its evolution (22, 23). In addition to vector transmission, *T. cruzi* is primarily maintained in nature by an usual primitive character of the enzootic cycle, which the ingestion of infected vectors by several mammal species, through predatory mechanisms of survival, keeping the parasite circulation (44). Orally transmitted acute Chagas' disease is currently the main route of transmission in northern South America and other Latin American countries (9, 44–46). Unlike the disease developed after vector-born transmission, patients infected by oral route develop a large number of signs and symptoms and present mortality rates highest (8%–35%) than patients infected by classical vectoral pathway (5%–10%) (47). These differences are probably related not only the greater efficiency of the parasite penetration in the gastric mucosa, but also usually the large quantity of parasites present in the ingested inoculum than those present in the excrement and that can penetrate through the skin (16).

In the present study, we utilized *T. cruzi* SC2005 strain (TcII), isolated from a patient during an oral outbreak of Chagas' disease in the south region of Brazil (34), to infect inbred mice from different

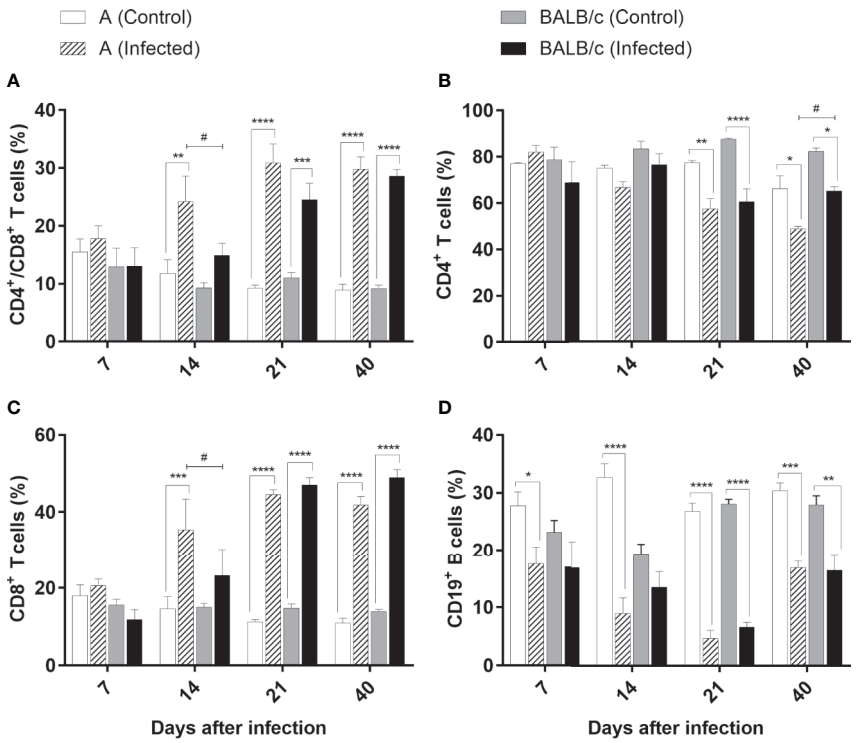

FIGURE 9 | Flow Cytometry analysis of the blood - Frequencies of $CD4^+/CD8^+$ T lymphocytes **(A)**, $CD4^+$T lymphocytes **(B)**, T $CD8^+$ T lymphocytes **(C)**, and $CD19^+$B lymphocytes **(D)** in blood samples obtained from uninfected and T. cruzi SC2005 intragastrically infected A and BALB/c mice. Data represent mean ± SEM of two independent experiments with six animals/group/day. Statistical analyses between groups were performed using Two-way Anova and Tukey multiple comparison test. Results were considered significant with $P < 0.05$ (*$P < 0.05$; **$P < 0.01$; ***$P < 0.001$; ****$P < 0.0001$). * represent differences between infected and control mice, # represent differences between A and BALB/c infected mice.

genetic backgrounds and compare the immunopathological alterations occurred after intragastric infection. BALB/c and A mice intragastrically infected by *T. cruzi* SC2005 showed high mortality rates, ranging from 10% to 25%, corroborating the highest mortality rates observed in patients orally infected. These mice developed a parasitemic profile similar to previously described in other studies in murine model using Swiss mice infected by *T. cruzi* strains from the same oral outbreak, showing double peaks of parasitemia, with the early low peak characteristic of biodeme type II (23, 48).

When we compare the effects of the oral infection between the two mouse strains, we observed significant differences in both parasitemia levels and percentages of survival. BALB/c mice were more susceptible to infection, showing highest parasitemia and mortality rates. Collins et al. (49) reported that the magnitude of the mucosal immune response developed after oral infection is the main factor which determines the parasite's fate of and the level of systemic parasitemia (49). The contribution of host genetics background in pathology caused by *T. cruzi* still unsolved and studies of genetic susceptibility to Chagas' disease are scarce. Marinho et al. (50) evaluated the pathology caused by Sylvio X10/4 *T. cruzi* in different inbred mouse strains chronically infected. C3H/HePAS mice exhibited higher cumulative mortality and pathology focused the heart, whereas A/J mice showed a mortality frequency similar to noninfected controls and liver alterations. showing that the genetic background of mice determines the development of chronic lesions (50). Since that in the present study we use the same *T. cruzi* strain to infect both mouse lineages, we also address that the differences in the parasitemia and mortality found in this study are influenced by immunological response developed by each mouse strain, which is determined by their genetic backgrounds.

Anemia is a common hematological alteration observed in infections caused by trypanosomes, being found in African trypanosomiasis (51) and in acute Chagas' disease. A profound anemia was described by Chagas in patients infected by *T. cruzi* (52). In the present work, both infected mouse strains showed hypochromic anemia after *T. cruzi* SC2005 intragastric infection. BALB/c mice presented a more pronounced hypochromic anemia at 14 dpi, when compared with A infected mice, which showed a higher decrease in RBC and Hgb at 21 dpi. Different mouse strains infected by *T. cruzi* also showed this hematological alteration (53). Nevertheless, the mechanisms responsible for this alteration are not clearly understood yet. Anemia could be caused by an impaired maturation of bone marrow precursors (54). The reduced number of blood cells and the impaired bone marrow function are associated with the lethality rate in acute *T. cruzi* infection (55). All these alterations in the blood and bone

marrow may be influenced by cytokines secretion, parasite, or cell-dependent cytotoxicity (56).

Several cytokines are related as suppressors of bone marrow activity, among them are TNF-α and IFN-γ (57–60). Binder et al. (57) have shown that the excessive production of TNF-α and IFN-γ appeared to promote damage in hematopoiesis of mice infected by lymphocytic choriomeningitis virus (LCMV). TNF-α has been also to be important as anemia mediator in studies with malaria (61). Inhibitory effects of TNF-α on erythropoiesis have been demonstrated in previous studies (60, 62), as well as during acute infection by *T. cruzi*, which the production of TNF-α by activated macrophages was correlated with a decrease in erythropoiesis (56). In our study both mouse strains infected by *T. cruzi* SC2005 produced high levels of TNF-α and IFN-γ at 14 days of infection, correlating with the decrease of RBC and Hgb. These results indicate that the anemia observed after *T. cruzi* infection can be associated with a depressed bone marrow function induced by TNF-α and IFN-γ.

Another factor that can contribute to anemia, is a reduced life span or sequestration of RBC by autoantibodies or other mechanisms, as described in other protozoan and viral infections (61, 63–67). In normal mice, the average life span of a red blood cell is 40 days (68). In the present study, BALB/c and A mice infected by *T. cruzi* SC2005 presented anemia earlier to this period, between 14 and 21 dpi, showing that *T. cruzi* infection reduces the life span of RBC contributing to anemia.

In consequence of the depressed bone marrow function, characterized by the insufficiency or poor quality of the blood elements produced, extramedullary hematopoiesis (EMH) can occur in adult mouse livers (69, 70). ECM does not occur in adult mice livers under normal physiological conditions, however, can occur under myelosuppression by various pathological lesions, including hemoglobinopathies, most commonly sickle cell anemia and thalassemia (71, 72). In our study, we observed the occurrence of extramedullary hematopoiesis, with the presence of megakaryocytes, immature hematopoietic cells and mitotic cells in the livers of *T. cruzi*-infected animals at 14 and 21 dpi. The occurrence of ECM in livers of Swiss Webster mice infected with the same *T. cruzi* strain have been previously described by us (23). Altogether, these findings corroborate the hypothesis that the anemia observed in mice infected with *T. cruzi* SC2005 is caused by an impairment in bone marrow function, induced by TNF-α and IFN-γ, which lead to occurrence of extramedullary hematopoiesis in mice livers as a compensatory mechanism.

Leukocytosis is another hematological alteration described after *T. cruzi* infection. In the present study both infected mouse strains showed a significant leukocytosis at 21 and 40 dpi, characterized by monocytosis and lymphocytosis, as well as by the presence of a lymphocytic atypia, which were associated with the parasitemia levels. Several works, using different experimental models, previously reported alterations in leukocyte counts associated with parasitemia levels. Beagle dogs infected by different *T. cruzi* strains showed a positive correlation between leukocytosis, lymphocytosis and parasitemia peaks (73, 74). The same correlation was found in cynomolgus macaque (*Macaca fascicularis*) naturally infected by *T cruzi* (75) and in Rhesus monkeys experimentally infected with *T cruzi* Colombian strain (76). Previous studies conducted by our group, also found a positive correlation between parasitemia levels and leukocytes counts in Swiss mice infected by *T. cruzi* SC2005. Contradictory results were obtained by other authors during experimental murine infection with *T. cruzi* CL strain. C3H infected-mice showed an exponential growth of parasites accompanied by leukopenia (54). Such dissimilarity in experimental data suggests that both the genetic background of experimental model and the *T. cruzi* strain may influence the impact on hematological characteristics of *T. cruzi* infection.

It is known that the increase of both Natural killer (NK) and $CD8^+$ T lymphocytes is characteristic of both acute and chronic *T cruzi* infections (77). Increased levels of these cells have been described as biomarkers for Chagas disease in humans and monkeys naturally infected by *T cruzi* (78). NK cells are an important source of IFN-γ, which activates macrophages to produce nitric oxide and subsequently control the parasite growth in acute *T cruzi* infections (77–79). Moreover, the cytotoxic activity of NK cells and $CD8^+$ T cells contributes to control parasite levels in the blood circulation, through the killing of parasites (78, 80, 81). As we described, BALB/c and A mice infected by *T. cruzi* SC2005 showed lymphocytosis (characterized by increase of $CD8^+$ T cells) at 21 and 40 dpi. The enhancement of these T cell subpopulations occurred at the parasitemia peak and persisted until the end of the infection when there was a reduction of parasite load. It is occur probably due to cytotoxic activity of these cells, as reported previously (75).

Inflammatory infiltration was found in many organs, and lymphocytes were the most frequently observed cell types. As observed in the blood, in the heart and liver there was an increase of $CD8^+$ T and $CD4^+/CD8^+$ T lymphocytes of both *T. cruzi*-infected mouse strains. $CD4^+/CD8^+$ double-positive T cells have been observed in individuals harboring infectious and autoimmune diseases, and chronic inflammatory disorders (82). Under normal conditions, these cell types are found in the thymus, where they undergo differentiation into mature $CD4^+$ and $CD8^+$ T cells. During *T. cruzi* infection, however, a deregulated cascade of proinflammatory cytokines significantly impaired this organ, leading to cell maturation in extrathymic organs such as the bone marrow and liver (83, 84). In the present study, the hematological findings showed a hypochromic microcytic anemia and lymphocytic atypia in infected mice during infection. This finding explains the circulation of $CD4^+/CD8^+$ T double-positive cells in the liver and blood, and indicates the maturation of the T lymphocytes expressing $CD4^+$ and $CD8^+$ co-receptors in the liver of A and BALB/c infected mice.

The performances of both $CD4^+$ and $CD8^+$ T cell subpopulations have been observed during *T. cruzi* infection, irrespective of the route of infection studied (23, 42, 49). $CD8^+$ T cells have been described as being of great importance for host resistance and effective control of the parasite outgrowth during acute and chronic infections (49, 81, 85). Studies indicate that $CD8^+$ T lymphocytes fail to restrain parasitemia and tissue parasitism in the absence of $CD4^+$ T cells (86). This

may occur because $CD4^+$ deficiency leads to an increase in tissue parasitism as a consequence of the overall reduction of host immune response, possibly due to the action of $CD4^+$ T lymphocytes in promoting the activation of macrophages and proliferation of $CD8^+$ T and B cells (87, 88). Therefore, these results show that both $CD4^+$ and $CD8^+$ T subpopulations are necessary for the development of protective immunity, being $CD8^+$ T cells more effective in develop an effector function against the parasite (89, 90). B cells are another cell type involved in *T. cruzi* infection. In addition to the secretion of antibodies, the role of B cells as antigen-presenting cells (APC), activating $CD8^+$ T cells was described in immunization studies (91). B cells are also related to the increased mobilization capacity of the inflammatory cells to the tissues and are fundamental to trigger Th1 response that favor the control of parasite growth (77, 92, 93).

In the present study, there was an increase of both $CD8^+$ T cells and $CD19^+$ B cells in the hepatic parenchyma, suggesting the development of APC functioning by the $CD19^+$ cells. However, A mice showed an early increase of these cells' frequencies (14 dpi) than BALB/c infected mice (21 dpi). The liver is the main organ involved in the defense against disseminating blood pathogen, regardless of portal of entry. On this way, immune surveillance by the liver is critical to host immunity and survival (94, 95). In *T. cruzi* infection, the liver is known to be a target tissue for the parasite and exert a role in clearance of blood trypomastigotes (96). Thus, the early presence of B and $CD8^+$ T cells in the liver observed in this work, indicates the importance of this organ in the parasite clearance and may explain why A mice had lower parasite load and mortality.

We also observe a decrease in the B lymphocyte frequencies in the heart and blood, and in $CD4^+$ T cells in the blood and heart of infected animals. This decrease is probably caused by the migration of this cell type to other sites affected by the infection. The subsequent return to normal levels is linked to the modulation of the local and systemic immune system. This regulation is often related to the severity of the clinical manifestations present, reflecting the redistribution and circulation of lymphocyte subtypes (23, 97).

The stomach has been described as the main region of *T. cruzi* invasion in the host (98, 99). In this study, the stomach of animals from both infected lineages presented intense inflammatory infiltrates. At 14 dpi, the presence of inflammatory cells in the muscular layer of the stomach of these animals, coincided with the largest amount of parasite DNA detected. In both strains, at 21 days of infection, the stomach was still very inflamed, but the presence of parasite DNA was very low. Although some authors describe the oral cavity, esophagus and palate as possible sites of parasite invasion (100, 101), the data from the present study indicate efficient migration, invasion and multiplication of parasite in the stomach of infected animals.

The heart of the infected BALB/c and A mice also showed intense immunopathological changes. Cases of death from acute Chagas disease are closely related to cardiac damage (3, 102). BALB/c mice showed largest cardiac involvement and a higher parasite load in this organ. The extensive damage of the heart plus the large number of parasite DNA and a late $CD8^+$ T cell response, corroborate to the highest number of deaths in this group.

In the liver, the presence of higher numbers of inflammatory cells around the vessels as well as in the parenchyma, indicates cellular extravasation and organ damage. In studies with BALB/c mice infected with the Tulahuén strain, the inflammatory infiltrate was not observed in the parenchyma region, but was located exclusively around the vessels (42). However, other studies describing the same findings of the present study. In independent studies using Swiss mice infected by Y or SC2005 *T. cruzi* strains, inflammatory infiltrates in parenchyma and around the liver vessels were also observed (23, 103). Sardinha et al. (96) described that the parasite and host cell interactions that occur during the initial infection by Y *T. cruzi* strain in C57BL/10 mice shows the presence of viable parasites in the liver, which are associated with the presence of focal inflammatory infiltrates in the liver parenchyma and in the perivascular spaces. These inflammatory infiltrates are composed by cells like macrophages, $CD4^+$ and $CD8^+$ T lymphocytes and natural killer cells, being important for parasite clearance, thus controlling parasitemia (96).

Paralleling parasitological, histological and immunophenotypical analysis, BALB/c and A infected-mice showed an enhancement of IFN-γ, TNF-α, and IL-6 Th1 cytokines in the serum, but A mice produce these cytokines earlier than BALB/c mice. These cytokines have a proinflammatory role and are involved in the parasite growth control and host resistance (104, 105). The importance of these cytokines in the response to *T. cruzi* infection has been described in several murine studies. The inhibition of IL-18 or 5-lipoxygenase in mice generated an increase in the levels of IL-12, IFN-γ, IL-1β, and IL-6, improving the resistance of mice to parasite growth during the acute phase of disease (106, 107). On the other hand, the reduced production of IFN-γ, IL-6, and TNF-α cytokines in C57BL/6 IL-17A knockout (IL-17A $^{-/-}$) mice infected with *T. cruzi* Tulahuén strain produced a more severe parasitemia and mortality, than observed in wild-type mice (108). *In vitro* studies using PBMC infected with *T. cruzi* Tulahuén strain indicate the action of IL-6 on cytotoxic cells, improving their survival and effector functions (105). These data reveal the great importance and the role of these cytokines in the control of parasite infection and mortality rates. In the present work, despite these proinflammatory cytokines were produced by both infected mice, A mice exhibited an earlier production of these cytokines, justifying the low parasitemia and mortality rate observed.

All the results point that the intragastric *T. cruzi* SC2005 infection produced a systemic response, that occur because *T. cruzi* spreads through the bloodstream, following the invasion and multiplication into the cells of different organs.

Although both mice infected strains exhibited the same profile of changes, A infected mice exhibited an early development of a cytotoxic cellular response, with a fast induction of $CD8^+$ T and proinflammatory cytokines production, with lower parasite load and mortality. On the other hand, in BALB/c infected mice the response to infection occurred later, after a considerable increase in parasitemia. This later cytotoxic and proinflammatory response favored the parasite multiplication and spread, and consequent higher mortality rate in these animals.

Altogether, these results point to the host genetic background shaping the response to infection and emphasize the importance of the earlier development of a cytotoxic cellular profile, with the production of proinflammatory cytokines for a less severe manifestation of Chagas disease.

DATA AVAILABILITY STATEMENT

All datasets presented in this study are included in the article/ **Supplementary Material**.

ETHICS STATEMENT

The animal study was reviewed and approved by the Ethics Committee for Animal Research of the Fundação Oswaldo Cruz (CEUA-FIOCRUZ), license LW 42/14.

AUTHOR CONTRIBUTIONS

CD and KC designed the study. CD, FC, DH, AB, and MP-M collected and analyzed the data. KC acquired the funding. CD and FC were in charge of the investigation. FC, CD, DH, and MP-M were in charge of the methodology. Project administration and supervision were done by KC. CD and FC wrote the original draft of the article. CD, FC, MP-M, AB, and KC wrote, reviewed and edited the article. All authors contributed to the article and approved the submitted version.

FUNDING

This work was supported by a grant from Instituto Oswaldo Cruz/Fundação Oswaldo Cruz. CD was a CAPES scholar. The funders had no role in the study design, data collection and analysis, decision to publish, or preparation of the manuscript.

ACKNOWLEDGMENTS

The authors would like to thank the Flow Cytometry Core Facilities of the Instituto Oswaldo Cruz/FIOCRUZ-RJ. We also thank Carla Cardozo Pinto de Arruda for comments on the manuscript, Sandy Santos Pereira for providing technical support, and Thaize Q. Chometon for operating the Cytoflex Flow Cytometer.

SUPPLEMENTARY MATERIAL

The Supplementary Material for this article can be found online at: https://www.frontiersin.org/articles/10.3389/fimmu.2020.566476/full#supplementary-material

SUPPLEMENTARY FIGURE 1 | Flow cytometry representative protocol. The gate strategy was performed, as follow: **(A)** to exclude cell aggregates from analyses, cells were gated on Singlets region in FSC-A vs. FSC-H dot-plot; **(B)** a SSC-A vs. FSC-A dot plot was created from Singlets gate and Monos region was defined; from Monos gate, **(C)** CD4+/CD3+ T lymphocytes; **(D)** CD8+/CD3+ T lymphocytes, **(E)** CD19+ B lymphocytes and **(F)** F4/80+ macrophages were determined. **(G)** CD8+/CD4+ double-positive T lymphocytes were defined from CD3+ gate in CD3 vs. FSC-A dot plot **(H)**. DN = Double Negatives.

REFERENCES

1. WHO. Chagas disease (American trypanosomiasis) (2020). Available at: https://www.who.int/health-topics/chagas-disease#tab=tab_1 (Accessed August 7, 2020).
2. Zingales B. Trypanosoma cruzi genetic diversity: Something new for something known about Chagas disease manifestations, serodiagnosis and drug sensitivity. *Acta Trop* (2018) 184:38–52. doi: 10.1016/j.actatropica.2017.09.017
3. Zingales B, Miles MA, Campbell DA, Tibayrenc M, Macedo AM, Teixeira MMG, et al. The revised Trypanosoma cruzi subspecific nomenclature: Rationale, epidemiological relevance and research applications. *Infect Genet Evol* (2012) 12:240–53. doi: 10.1016/j.meegid.2011.12.009
4. Lima L, Espinosa-Álvarez O, Ortiz PA, Trejo-Varón JA, Carranza JC, Pinto CM, et al. Genetic diversity of Trypanosoma cruzi in bats, and multilocus phylogenetic and phylogeographical analyses supporting Tcbat as an independent DTU (discrete typing unit). *Acta Trop* (2015) 151:166–77. doi: 10.1016/j.actatropica.2015.07.015
5. Zingales B, Andrade SG, Briones MRS, Campbell DA, Chiari E, Fernandes O, et al. A new consensus for Trypanosoma cruzi intraspecific nomenclature: Second revision meeting recommends TcI to TcVI. *Mem Inst Oswaldo Cruz* (2009) 104:1051–4. doi: 10.1590/S0074-02762009000700021
6. Gascon J, Bern C, Pinazo MJ. Chagas disease in Spain, the United States and other non-endemic countries. *Acta Trop* (2010) 115:22–7. doi: 10.1016/j.actatropica.2009.07.019
7. Molyneux DH, Savioli L, Engels D. Neglected tropical diseases: progress towards addressing the chronic pandemic. *Lancet* (2017) 389:312–25. doi: 10.1016/S0140-6736(16)30171-4
8. World Health Organization. Global distribution of cases of Chagas disease, based on official estimates, 2018 (2018). Available at: https://www.who.int/docs/default-source/ntds/chagas-disease/chagas-2018-cases.pdf?sfvrsn=f4e94b3b_2 (Accessed August 7, 2020).
9. Shikanai-Yasuda MA, Carvalho NB. Oral transmission of chagas disease. *Clin Infect Dis* (2012) 54:845–52. doi: 10.1093/cid/cir956
10. Secretaria de Vigilância em Saúde. Boletim Epidemiológico - Doença de Chagas aguda no Brasil: série histórica de 2000 a 2013. *Ministério da Saúde* (2015) 46:1–9.
11. Lidani KCF, Andrade FA, Bavia L, Damasceno FS, Beltrame MH, Messias-Reason IJ, et al. Chagas Disease: From Discovery to a Worldwide Health Problem. *Front Public Health* (2019) 7:166. doi: 10.3389/fpubh.2019.00166
12. Marcili A, Lima L, Cavazzana M, Junqueira ACV, Veludo HH, Maia Da Silva F, et al. A new genotype of Trypanosoma cruzi associated with bats evidenced by phylogenetic analyses using SSU rDNA, cytochrome b and Histone H2B genes and genotyping based on ITS1 rDNA. *Parasitology* (2009) 136:641–55. doi: 10.1017/S0031182009005861
13. Monteiro WM, Magalhães LK, Santana Filho FS, Borborema M, Silveira H, Barbosa MDGV. Trypanosoma cruzi TcIII/Z3 genotype as agent of an outbreak of Chagas disease in the Brazilian Western Amazonia: Short Communication. *Trop Med Int Health* (2010) 15:1049–51. doi: 10.1111/j.1365-3156.2010.02577.x
14. Monteiro WM, Magalhães LKC, de Sá ARN, Gomes ML, Toledo MJ de O, Borges L, et al. Trypanosoma cruzi IV causing outbreaks of acute chagas disease and infections by different haplotypes in the Western Brazilian Amazonia. *PLoS One* (2012) 7(7):e41284. doi: 10.1371/journal.pone.0041284
15. Benchimol Barbosa PR. The oral transmission of Chagas' disease: An acute form of infection responsible for regional outbreaks. *Int J Cardiol* (2006) 112:132–3. doi: 10.1016/j.ijcard.2005.11.087
16. Filigheddu MT, Górgolas M, Ramos JM. Enfermedad de Chagas de transmisión oral. *Med Clin (Barc)* (2016) 148:125–31. doi: 10.1016/j.medcli.2016.10.038

17. Rueda K, Trujillo JE, Carranza JC, Vallejo GA. Transmisión oral de Trypanosoma cruzi: una nueva situación epidemiológica de la enfermedad de Chagas en Colombia y otros países suramericanos. *Biomédica* (2014) 34:631–41. doi: 10.7705/biomedica.v34i4.2204
18. Macedo AM, Oliveira RP, Pena SDJ. Chagas disease: role of parasite genetic variation in pathogenesis. *Expert Rev Mol Med* (2002) 4:1–16. doi: 10.1017/s1462399402004118
19. Macedo AM, Machado CR, Oliveira RP, Pena SDJ. Trypanosoma cruzi: Genetic structure of populations and relevance of genetic variability to the pathogenesis of chagas disease. *Mem Inst Oswaldo Cruz* (2004) 99:1–12. doi: 10.1590/S0074-02762004000100001
20. Buscaglia CA, Di Noia JM. Trypanosoma cruzi clonal diversity and the epidemiology of Chagas' disease. *Microbes Infect* (2003) 5:419–27. doi: 10.1016/S1286-4579(03)00050-9
21. Campbell D, Westenberger S, Sturm N. The Determinants of Chagas Disease: Connecting Parasite and Host Genetics. *Curr Mol Med* (2004) 4:549–62. doi: 10.2174/1566524043360249
22. Lewis MD, Francisco AF, Jayawardhana S, Langston H, Taylor MC, Kelly JM. Imaging the development of chronic Chagas disease after oral transmission. *Sci Rep* (2018) 8(1):11292. doi: 10.1038/s41598-018-29564-7
23. Domingues CS, Hardoim DJ, Souza CSF, Cardoso FO, Mendes VG, Previtalli-Silva H, et al. Oral outbreak of chagas disease in santa catarina, Brazil: Experimental evaluation of a patient's strain. *PLoS One* (2015) 10:1–18. doi: 10.1371/journal.pone.0122566
24. Silva GK, Cunha LD, Horta CV, Silva ALN, Gutierrez FRS, Silva JS, et al. A Parent-of-Origin Effect Determines the Susceptibility of a Non-Informative F1 Population to Trypanosoma cruzi Infection In Vivo. *PLoS One* (2013) 8 (2):e56347. doi: 10.1371/journal.pone.0056347
25. Hardoim DJ. *Imunopatologia da infecção por Trypanosoma cruzi em camundongos CBA e C57BL/10 infectados pela vias intragástrica e intraperitoneal. [master's thesis]*. Rio de Janeiro (RJ: Instituto Oswaldo Cruz/Fundação Oswaldo Cruz (2014).
26. Ferreira BL, Ferreira ÉR, de Brito MV, Salu BR, Oliva MLV, Mortara RA, et al. BALB/c and C57BL/6 mice cytokine responses to Trypanosoma cruzi infection are independent of parasite strain infectivity. *Front Microbiol* (2018) 9:553. doi: 10.3389/fmicb.2018.00553
27. Andrade LO, Machado CRS, Chiari E, Pena SDJ, Macedo AM. Trypanosoma cruzi: Role of host genetic background in the differential tissue distribution of parasite clonal populations. *Exp Parasitol* (2002) 100:269–75. doi: 10.1016/S0014-4894(02)00024-3
28. Freitas JM, Andrade LO, Pires SF, Lima R, Chiari E, Santos RR, et al. The MHC gene region of murine hosts influences the differential tissue tropism of infecting Trypanosoma cruzi strains. *PLoS One* (2009) 4(4):e5113. doi: 10.1371/journal.pone.0005113
29. Deghaide NHS, Dantas RO, Donadi EA. HLA class I and II profiles of patients presenting with Chagas' disease. *Dig Dis Sci* (1998) 43:246–52. doi: 10.1023/A:1018829600200
30. Layrisse Z, Fernandez MT, Montagnani S, Matos M, Balbas O, Herrera F, et al. HLA-C*03 is a risk factor for cardiomyopathy in Chagas disease. *Hum Immunol* (2000) 61:925–9. doi: 10.1016/S0198-8859(00)00161-0
31. Cruz-Robles D, Reyes PA, Monteón-Padilla VM, Ortiz-Muñiz AR, Vargas-Alarcón G. MHC class I and class II genes in mexican patients with Chagas disease. *Hum Immunol* (2004) 65:60–5. doi: 10.1016/j.humimm.2003.10.008
32. Cunha-Neto E, Chevillard C. Chagas disease cardiomyopathy: Immunopathology and genetics. *Mediators Inflamm* (2014) 2014:1–11. doi: 10.1155/2014/683230
33. Chevillard C, Nunes JPS, Frade AF, Almeida RR, Pandey RP, Nascimento MS, et al. Disease Tolerance and Pathogen Resistance Genes May Underlie Trypanosoma cruzi Persistence and Differential Progression to Chagas Disease Cardiomyopathy. *Front Immunol* (2018) 9:2791. doi: 10.3389/fimmu.2018.02791
34. Steindel M, Kramer Pacheco L, Scholl D, Soares M, de Moraes MH, Eger I, et al. Characterization of Trypanosoma cruzi isolated from humans, vectors, and animal reservoirs following an outbreak of acute human Chagas disease in Santa Catarina State, Brazil. *Diagn Microbiol Infect Dis* (2008) 60:25–32. doi: 10.1016/j.diagmicrobio.2007.07.016
35. da Silva CV, Luquetti AO, Rassi A, Mortara RA. Involvement of Ssp-4-related carbohydrate epitopes in mammalian cell invasion by Trypanosoma cruzi amastigotes. *Microbes Infect* (2006) 8:2120–9. doi: 10.1016/j.micinf.2006.03.016
36. Camargo EP. Growth and differentiation in Trypanosoma cruzi. I. Origin of metacyclic trypanosomes in liquid media. *Rev Inst Med Trop Sao Paulo* (1964) 6:93–100.
37. Hoff R. Method for counting and concentrating living Trypanosoma cruzi in blood lysed with ammonium-chloride. *J Parasitol* (1974) 60:527–8. doi: 10.2307/3278377
38. Pizzi T, Prager R. Estabilización de la virulencia de una cepa de Trypanosoma cruzi por pasaje seriado en ratones de constitución genética uniforme: análises cuantitativo del curso de la infección. *Biológica* (1952) 16:3–12.
39. Sambrook J, Russell DW. Purification of Nucleic Acids by Extraction with Phenol:Chloroform. *Cold Spring Harb Protoc* (2006) 2006:pdb.prot4455. doi: 10.1101/pdb.prot4455
40. Piron M, Fisa R, Casamitjana N, López-Chejade P, Puig L, Vergés M, et al. Development of a real-time PCR assay for Trypanosoma cruzi detection in blood samples. *Acta Trop* (2007) 103:195–200. doi: 10.1016/j.actatropica.2007.05.019
41. Giulietti A, Overbergh L, Valckx D, Decallonne B, Bouillon R, Mathieu C. An overview of real-time quantitative PCR: Applications to quantify cytokine gene expression. *Methods* (2001) 25:386–401. doi: 10.1006/meth.2001.1261
42. Barreto-de-Albuquerque J, Silva-dos-Santos D, Pérez AR, Berbert LR, de Santana-van-Vliet E, Farias-de-Oliveira DA, et al. Trypanosoma cruzi infection through the oral route promotes a severe infection in mice: New disease form from an old infection? *PLoS Negl Trop Dis* (2015) 9(6): e0003849. doi: 10.1371/journal.pntd.0003849
43. Andersson J, Örn A, Sunnemark D. Chronic murine Chagas' disease: The impact of host and parasite genotypes. *Immunol Lett* (2003) 86:207–12. doi: 10.1016/S0165-2478(03)00019-1
44. Coura JR. The main sceneries of chagas disease transmission. The vectors, blood and oral transmissions - A comprehensive review. *Mem Inst Oswaldo Cruz* (2015) 110:277–82. doi: 10.1590/0074-0276140362
45. Santos EF, Silva ÂAO, Leony LM, Freitas NEM, Daltro RT, Regis-Silva CG, et al. Acute Chagas disease in Brazil from 2001 to 2018: A nationwide spatiotemporal analysis. *PLoS Negl Trop Dis* (2020) 14:e0008445. doi: 10.1371/journal.pntd.0008445
46. dos Santos VRC, de Meis J, Savino W, Andrade JAA, Vieira JR dos S, Coura JR, et al. Acute chagas disease in the state of Pará, amazon region: Is it increasing? *Mem Inst Oswaldo Cruz* (2018) 113:1–6. doi: 10.1590/0074-02760170298
47. Rassi A, Rassi A, Marin-Neto JA. Chagas disease. *Lancet* (2010) 375:1388–402. doi: 10.1016/S0140-6736(10)60061-X
48. Andrade SG, Campos RF, Steindel M, Guerreiro ML, Magalhães JB, de Almeida MC, et al. Biological, biochemical and molecular features of Trypanosoma cruzi strains isolated from patients infected through oral transmission during a 2005 outbreak in the state of Santa Catarina, Brazil: Its correspondence with the new T. cruzi taxonomy consensus (2009). *Mem Inst Oswaldo Cruz* (2011) 106:948–56. doi: 10.1590/S0074-02762011000800009
49. Collins MH, Craft JM, Bustamante JM, Tarleton RL. Oral exposure to Trypanosoma cruzi elicits a systemic CD8+ T cell response and protection against heterotopic challenge. *Infect Immun* (2011) 79:3397–406. doi: 10.1128/IAI.01080-10
50. Marinho CRF, Bucci DZ, Dagli MLZ, Bastos KRB, Grisotto MG, Sardinha LR, et al. Pathology Affects Different Organs in Two Mouse Strains Chronically Infected by A Trypanosoma cruzi Clone: A Model for Genetic Studies of Chagas' Disease. *Infect Immun* (2004) 72:2350–7. doi: 10.1128/IAI.72.4.2350-2357.2004
51. Ikede BO, Lule M, Terry RJ. Anaemia in trypanosomiasis: mechanisms of erythrocyte destruction in mice infected with Trypanosoma congolense or T. brucei. *Acta Trop* (1977) 34(1):53–60.
52. Chagas C. Nova tripanosomiaze humana. *Mem Inst Oswaldo Cruz* (1909) 1:3–62. doi: 10.1590/S0074-02761909000200008
53. Cardoso JE, Brener Z. Hematological changes in mice experimentally infected with Trypanosoma cruzi. *Mem Inst Oswaldo Cruz* (1980) 75:97–104. doi: 10.1590/S0074-02761980000200009
54. Marcondes MCG, Borelli P, Yoshida N, Russo M. Acute Trypanosoma cruzi infection is associated with anemia, thrombocytopenia, leukopenia, and bone marrow hypoplasia: Reversal by nifurtimox treatment. *Microbes Infect* (2000) 2:347–52. doi: 10.1016/S1286-4579(00)00333-6

55. Andrade SG, Rassi A, Magalhaes JB, Ferriolli Filho F, Luquetti AO. Specific chemoterapy of Chagas disease: a comparison between the response in patients and experimental animals inoculated with the same strain. *Trans R Soc Trop Med Hyg* (1992) 86:624–6. doi: 10.1016/0035-9203(92)90156-7
56. Malvezi AD, Cecchini R, De Souza F, Tadokoro CE, Rizzo LV, Pinge-Filho P. Involvement of nitric oxide (NO) and TNF-α in the oxidative stress associated with anemia in experimental Trypanosoma cruzi infection. *FEMS Immunol Med Microbiol* (2004) 41:69–77. doi: 10.1016/j.femsim.2004.01.005
57. Binder D, Van Den Broek MF, Kägi D, Bluethmann H, Fehr J, Hengartner H, et al. Aplastic anemia rescued by exhaustion of cytokine-secreting CD8+ T cells in persistent infection with lymphocytic choriomeningitis virus. *J Exp Med* (1998) 187:1903–20. doi: 10.1084/jem.187.11.1903
58. Ben D, Chen M. MM. Recombinant Tumor Necrosis Factor enhances the proliferative responsiveness of murine peripheral macrophages to Macrophage-Colony Stimulating Factor but inhibits their proliferative respon- siveness to Granulocyte-Macrophage-Colony Stimulating Factor. *Blood* (1990) 75:1627–32. doi: 10.1182/blood.V75.8.1627.bloodjournal7581627
59. Moldawer LL, Marano MA, Wei H, Fong Y, Silen ML, Kuo G, et al. Cachectin/tumor necrosis factor-α alters red blood cell kinetics and induces anemia in vivo. *FASEB J* (1989) 3:1637–43. doi: 10.1096/fasebj.3.5.2784116
60. Ulich TR, Shin SS, del Castillo J. Haematologic effects of TNF. *Res Immunol* (1993) 144(5):347–54. doi: 10.1016/s0923-2494(93)80079-e
61. Miller LH, Good MF, Milon G, Miller LH, Good MF. MG. Malaria pathogenesis. *Sci (80-)* (1994) 264:1878–83. doi: 10.1126/science.8009217
62. Young HA, Klinman DM, Reynolds DA, Grzegorzewski KJ, Nii A, Ward JM, et al. Bone marrow and thymus expression of interferon-gamma results in severe B-cell lineage reduction, T-cell lineage alterations, and hematopoietic progenitor deficiencies. *Blood* (1997) 89:583–95. doi: 10.1182/blood.V89.2.583
63. Thomsen AR, Pisa P, Bro-Jorgensen K. KR. Mechanisms of lymphocytic choriomeningitis virus induced hemopoietic dysfunction. *J Virol* (1986) 59:428–33. doi: 10.1128/JVI.59.2.428-433.1986
64. Rakusan TA. Inhibition of colony formation by human cytomegovirus in vitro. *J Infect Dis* (1989) 159:127–30. doi: 10.1093/infdis/159.1.127
65. Kaloutsi V, Kohlmeyer V, Maschet H, Nafe RCH, Amor A. GA. Comparison of bone marrow and hematological findings in patients with human immunodeficiency virus infection and those with myelodisplastic syndromes and infectious diseases. *Am J Clin Pathol* (1994) 101:123–9. doi: 10.1093/ajcp/101.2.123
66. Watier H, Verwaerde C, Landau I, Werner EFJ, Capron A. AC. T cell-dependent immunity and thrombocytopenia in rats infected with Plasmodium chabaudi. *Infect Immun* (1992) 60:136–42. doi: 10.1128/IAI.60.1.136-142.1992
67. Davis CE, Robbins RS, Weller RD. BAI. Thrombocytopenia in experimental trypanosomiasis. *J Clin Invest* (1974) 53:1359–67. doi: 10.1172/JCI107684
68. Van Putten LM. The life span of red cells in the rat and the mouse as determined by labeling with DFP32 in vivo. *Blood* (1958) 13:789–94. doi: 10.1182/blood.v13.8.789.789
69. Ploemacher RE, van Soest PL. Morphological investigation on phenylhydrazine-induced erythropoiesis in the adult mouse liver. *Cell Tissue Res* (1977) 178:435–61. doi: 10.1007/BF00219567
70. Cardier JE, Barberá-Guillem E. Extramedullary hematopoiesis in the adult mouse liver is associated with specific hepatic sinusoidal endothelial cells. *Hepatology* (1997) 26:165–75. doi: 10.1002/hep.510260122
71. Georgiades CS, Neyman EG, Francis IR, Sneider MB, Fishman EK. Typical and atypical presentations of extramedullary hemopoiesis. *Am J Roentgenol* (2002) 179:1239–43. doi: 10.2214/ajr.179.5.1791239
72. Roberts AS, Shetty AS, Mellnick VM, Pickhardt PJ, Bhalla S, Menias CO. Extramedullary haematopoiesis: radiological imaging features. *Clin Radiol* (2016) 71:807–14. doi: 10.1016/j.crad.2016.05.014
73. Marcos P, Guedes M, Veloso VM, Wilson T, Mineo P, Santiago-Silva J, et al. Hematological alterations during experimental canine infection by Trypanosoma cruzi Alterações hematológicas durante a infecção canina experimental por Trypanosoma cruzi. Available at: www.cbpv.com.br/rbpv (Accessed August 17, 2020).
74. Barr SC, Gossett KA, Klei TR. Clinical, clinicopathologic, and parasitologic observations of trypanosomiasis in dogs infected with North American Trypanosoma cruzi isolates. *Am J Vet Res* (1991) 52(6):954–60.
75. Henderson SE, Pfeiffer SC, Novak J, Peace TA. Large granular lymphocytosis in a cynomolgus macaque (Macaca fascicularis) with a subclinical Trypanosoma cruzi infection. *Vet Clin Pathol* (2020) 00:1–7. doi: 10.1111/vcp.12879
76. Bonecini-Almeida M, Galvão-Castro B, Pessoa HR, Pirmez C, Laranja F. Experimental Chagas's disease in Rhesus monkeys. I. Clinical, parasitological, hematological and anatomo-pathological studies in the acute and indeterminate phase of the disease. *Mem Inst Oswaldo Cruz* (1990) 85:163–71. doi: 10.1590/S0074-02761990000200004
77. Cardillo F, De Pinho RT, Antas PRZ, Mengel J. Immunity and immune modulation in Trypanosoma cruzi infection. *Pathog Dis* (2015) 73(9):1–8. doi: 10.1093/femspd/ftv082
78. Sathler-Avelar R, Vitelli-Avelar DM, Mattoso-Barbosa AM, Perdigão-de-Oliveira M, Costa RP, Elói-Santos SM, et al. Phenotypic Features of Circulating Leukocytes from Non-human Primates Naturally Infected with Trypanosoma cruzi Resemble the Major Immunological Findings Observed in Human Chagas Disease. *PLoS Negl Trop Dis* (2016) 10(1):e0004302. doi: 10.1371/journal.pntd.0004302
79. Vitelli-Avelar DM, Sathler-Avelar R, Mattoso-Barbosa AM, Gouin N, Perdigão-de-Oliveira M, Valério-dos-Reis L, et al. Cynomolgus macaques naturally infected with Trypanosoma cruzi-I exhibit an overall mixed pro-inflammatory/modulated cytokine signature characteristic of human Chagas disease. *PLoS Negl Trop Dis* (2017) 11(2):e0005233. doi: 10.1371/journal.pntd.0005233
80. Lieke T, Graefe SEB, Klauenberg U, Fleischer B, Jacobs T. NK cells contribute to the control of Trypanosoma cruzi infection by killing free parasites by perforin-independent mechanisms. *Infect Immun* (2004) 72:6817–25. doi: 10.1128/IAI.72.12.6817-6825.2004
81. Tarleton RL. CD8+ T cells in Trypanosoma cruzi infection. *Semin Immunopathol* (2015) 37:233–8. doi: 10.1007/s00281-015-0481-9
82. Pérez AR, Morrot A, Berbert LR, Terra-Granado E, Savino W. Extrathymic CD4+CD8+ lymphocytes in Chagas disease: possible relationship with an immunoendocrine imbalance. *Ann N Y Acad Sci* (2012) 1262:27–36. doi: 10.1111/j.1749-6632.2012.06627.x
83. Caselna TTT, Cruvinel WM, Mesquita Junior D, Araújo JAP, de Souza AWS, Andrade LEC, et al. da imunologia aos imunobiológicos. *Sinopse Reumatol* (2008) 2:35–57.
84. Pérez AR, Roggero E, Nicora A, Palazzi J, Besedovsky HO, del Rey A, et al. Thymus atrophy during Trypanosoma cruzi infection is caused by an immuno-endocrine imbalance. *Brain Behav Immun* (2007) 21:890–900. doi: 10.1016/j.bbi.2007.02.004
85. Acosta Rodríguez EV, Araujo Furlan CL, Fiocca Vernengo F, Montes CL, Gruppi A. Understanding CD8+ T Cell Immunity to Trypanosoma cruzi and How to Improve It. *Trends Parasitol* (2019) 35:899–917. doi: 10.1016/j.pt.2019.08.006
86. Padilla A, Xu D, Martin D, Tarleton R. Limited role for CD4+ T-cell help in the initial priming of Trypanosoma cruzi-specific CD8+ T cells. *Infect Immun* (2007) 75:231–5. doi: 10.1128/IAI.01245-06
87. Gonçalves Da Costa SC, Calabrese KS, Zaverucha Do Valle T, Lagrange PH. Trypanosoma cruzi: Infection patterns in intact and athymic mice of susceptible and resistant genotypes. *Histol Histopathol* (2002) 17:837–44. doi: 10.14670/HH-17.837
88. Rottenberg ME, Riarte A, Sporrong L, Altcheh J, Petray P, Ruiz AM, et al. Outcome of infection with different strains of Trypanosoma cruzi in mice lacking CD4 and/or CD8. *Immunol Lett* (1995) 45:53–60. doi: 10.1016/0165-2478(94)00221-C
89. Sullivan NL, Eickhoff CS, Sagartz J, Hoft DF. Deficiency of Antigen-Specific B Cells Results in Decreased Trypanosoma cruzi Systemic but Not Mucosal Immunity Due to CD8 T Cell Exhaustion. *J Immunol* (2015) 194:1806–18. doi: 10.4049/jimmunol.1303163
90. Sullivan NL, Eickhoff CS, Zhang X, Giddings OK, Lane TE, Hoft DF. Importance of the CCR5–CCL5 Axis for Mucosal Trypanosoma cruzi Protection and B Cell Activation. *J Immunol* (2011) 187:1358–68. doi: 10.4049/jimmunol.1100033
91. Hoft DF, Eickhoff CS, Giddings OK, Vasconcelos JRC, Rodrigues MM. Trans -Sialidase Recombinant Protein Mixed with CpG Motif-Containing Oligodeoxynucleotide Induces Protective Mucosal and Systemic Trypanosoma cruzi Immunity Involving CD8 + CTL and B Cell-Mediated Cross-Priming. *J Immunol* (2007) 179:6889–900. doi: 10.4049/jimmunol.179.10.6889

92. Cardillo F, Postol E, Nihei J, Aroeira LS, Nomizo A, Mengel J. B cells modulate T cells so as to favour T helper type 1 and CD8 + T-cell responses in the acute phase of Trypanosoma cruzi infection. *Immunology* (2007) 122:584–95. doi: 10.1111/j.1365-2567.2007.02677.x
93. Arantes JM, Francisco AF, de Abreu Vieira PM, Silva M, Araújo MSS, de Carvalho AT, et al. Trypanosoma cruzi: Desferrioxamine decreases mortality and parasitemia in infected mice through a trypanostatic effect. *Exp Parasitol* (2011) 128:401–8. doi: 10.1016/j.exppara.2011.05.011
94. Jenne CN, Kubes P. Immune surveillance by the liver. *Nat Immunol* (2013) 14:996–1006. doi: 10.1038/ni.2691
95. Kubes P, Jenne C. Immune Responses in the Liver. *Annu Rev Immunol* (2018) 36:1–31. doi: 10.1146/annurev-immunol-051116-052415
96. Sardinha LR, Mosca T, Elias RM, do Nascimento RS, Gonçalves LA, Bucci DZ, et al. The Liver Plays a Major Role in Clearance and Destruction of Blood Trypomastigotes in Trypanosoma cruzi Chronically Infected Mice. *PLoS Negl Trop Dis* (2010) 4:e578. doi: 10.1371/journal.pntd.0000578
97. Dominguez MR, Ersching J, Lemos R, Machado AV, Bruna-Romero O, Rodrigues MM, et al. Re-circulation of lymphocytes mediated by sphingosine-1-phosphate receptor-1 contributes to resistance against experimental infection with the protozoan parasite Trypanosoma cruzi. *Vaccine* (2012) 30:2882–91. doi: 10.1016/j.vaccine.2012.02.037
98. Maeda FY, Clemente TM, Macedo S, Cortez C, Yoshida N. Host cell invasion and oral infection by Trypanosoma cruzi strains of genetic groups TcI and TcIV from chagasic patients. *Parasit Vectors* (2016) 9(189):1–12. doi: 10.1186/s13071-016-1455-z
99. Filigheddu MT, Górgolas M, Ramos JM. Orally-transmitted Chagas disease. *Med Clin (Barc)* (2017) 148:125–31. doi: 10.1016/j.medcli.2016.10.038
100. Añez N, Crisante G, Rojas A, Dávila D. Brote de enfermedad de Chagas agudo de posible transmisión oral en Mérida, Venezuela. *Bol Malariol Salud Ambient* (2013) 53:1–11.
101. Silva-dos-Santos D, Barreto-de-Albuquerque J, Guerra B, Moreira OC, Berbert LR, Ramos MT, et al. Unraveling Chagas disease transmission through the oral route: Gateways to Trypanosoma cruzi infection and target tissues. *PLoS Negl Trop Dis* (2017) 11(4):e0005507. doi: 10.1371/journal.pntd.0005507
102. de Góes Costa E, dos Santos SO, Sojo-Milano M, Amador ECC, Tatto E, Souza DSM, et al. Acute Chagas Disease in the Brazilian Amazon: Epidemiological and clinical features. *Int J Cardiol* (2017) 235:176–8. doi: 10.1016/j.ijcard.2017.02.101
103. Arantes JM. *Influência da utilização da desferrioxamina, quelante de ferro, sobre o curso da infecção pelo Trypanosoma cruzi em camundongos. [master's thesis]*. Ouro Preto (MG: Universidade Federal de Ouro Preto (2006).
104. Gutierrez FRS, Guedes PMM, Gazzinelli RT, Silva JS. The role of parasite persistence in pathogenesis of Chagas heart disease. *Parasite Immunol* (2009) 31:673–85. doi: 10.1111/j.1365-3024.2009.01108.x
105. Sanmarco LM, Visconti LM, Eberhardt N, Ramello MC, Ponce NE, Spitale NB, et al. IL-6 improves the nitric oxide-induced cytotoxic CD8+ T cell dysfunction in human chagas disease. *Front Immunol* (2016) 7(626):1–12. doi: 10.3389/fimmu.2016.00626
106. Canavaci AMC, Sorgi CA, Martins VP, Morais FR, De Sousa ÉVG, Trindade BC, et al. The acute phase of trypanosoma cruzi infection is attenuated in 5-lipoxygenase-deficient mice. *Mediators Inflamm* (2014) 893634. doi: 10.1155/2014/893634
107. Esper L, Utsch L, Soriani FM, Brant F, Esteves Arantes RM, Campos CF, et al. Regulatory effects of IL-18 on cytokine profiles and development of myocarditis during Trypanosoma cruzi infection. *Microbes Infect* (2014) 16:481–90. doi: 10.1016/j.micinf.2014.03.007
108. Miyazaki Y, Hamano S, Wang S, Shimanoe Y, Iwakura Y, Yoshida H. IL-17 Is Necessary for Host Protection against Acute-Phase Trypanosoma cruzi Infection. *J Immunol* (2010) 185:1150–7. doi: 10.4049/jimmunol.0900047

Conflict of Interest: The authors declare that the research was conducted in the absence of any commercial or financial relationships that could be construed as a potential conflict of interest.